京都大学臨界集合体実験装置での加速器駆動システムにおける高速中性子スペクトル炉心の実験ベンチマーク

Experimental Benchmarks of Medium-Fast Spectrum Core (EE1 Core) in Accelerator-Driven System at Kyoto University Critical Assembly

著者： 卞　哲浩

Author ：Cheol Ho Pyeon

Preface

The main objective of these benchmarks is to contribute to research and development of neutronics on fast neutron spectrum cores in ADS through the experimental data with the use of differing external neutron (14 MeV neutrons generated by D-T reactions; spallation neutrons generated by 100 MeV protons and Pb-Bi target), carried out at the Kyoto University Critical Assembly (KUCA) A-core.

Special thanks are due the KUCA and the fixed-filed alternative gradient (FFAG) accelerator staff for support and patience throughout a series of ADS experiments carried out at KUCA.

<div align="right">Cheol Ho Pyeon</div>

May 2020

要　旨

　この実験ベンチマーク問題は、KUCA の A 架台において行われた 2 種類の異なる外部中性子源（コッククロフト・ウォルトン加速器の DT 反応から 14 MeV 中性子、または FFAG 加速器と Pb-Bi ターゲットを組み合わせて得られる核破砕中性子）を用いた実験を通して、ADS における高速中性子スペクトル炉心の中性子特性に関する基礎研究の発展に貢献することを目的としている。

　最後に、KUCA において ADS 実験を準備および運転にご協力をいただいた KUCA および FFAG 加速器のスタッフに心から感謝の意を表します。

<div align="right">

卞　哲浩

2020 年 5 月

</div>

Contents

Experimental Benchmarks of Medium-Fast Spectrum Core (EE1 Core) in Accelerator-Driven System at Kyoto University Critical Assembly

目　次

京都大学臨界集合体実験装置での加速器駆動システムにおける高速中性子スペクトル炉心（EE1 炉心）の実験ベンチマーク

Experimental Benchmarks of Medium-Fast Spectrum Core (EE1 Core) in Accelerator-Driven System at Kyoto University Critical Assembly

Institute for Integrated Radiation and Nuclear Science, Kyoto University, Japan

Cheol Ho Pyeon

Study I

Kinetic Parameters

1. Collaborative Work Specifications

1-1 Introduction

The accelerator-driven system (ADS) was developed for producing energy and for transmuting minor actinides and long-lived fission products. ADS has attracted worldwide attention in recent years because of its superior safety characteristics and potential for burning plutonium and nuclear waste. An outstanding advantage of its use is the anticipated absence of reactivity accidents, provided sufficient subcriticality is ensured. At the Institute for Integrated Radiation and Nuclear Science, Kyoto University (KURNS; former Kyoto University Research Reactor Institute: KURRI) [1]-[2], a series of experiments on ADS was launched in fiscal 2003 at the Kyoto University Critical Assembly (KUCA) [3]-[26], with sights on a future plan (**K**umatori **A**ccelerator Driven **R**eactor **T**est Facility **&** Innovation Research **Labo**ratory: Kart & Lab. Project). A new accelerator was attached to the KUCA facility in March 2008, and the high-energy neutrons generated by the interaction of 100 MeV protons with tungsten target was injected into KUCA. The new accelerator is called the fixed-field alternating gradient (FFAG) [27]-[28] accelerator of the synchrotron type developed by the High Energy Accelerator Research Organization (KEK) in Japan.

The experimental studies on ADS had been conducted for nuclear transmutation analyses with the combined use of KUCA and the FFAG accelerator, KURNS. The ADS experiments [17]-[26] with 100 MeV protons obtained from the FFAG accelerator had been carried out to investigate the neutron characteristics of ADS, and the static and kinetic parameters were accurately analyzed through both the measurements and the Monte Carlo simulations of reactor physics parameters, including the reaction rates, the neutron spectrum, the neutron multiplication, the neutron decay constants and the subcriticality. In addition to the uranium-loaded cores, the spallation neutrons generated by 100 MeV proton beams from the FFAG accelerator had been also injected into the thorium-loaded cores [21]-[22] to conduct the feasibility studies on the thorium-loaded ADS through the experimental analyses of the static conditions and kinetic behaviors.

In this study, attention was paid to the neutron characteristics of medium-fast spectrum in the solid-moderated and solid-reflected core (termed EE1 core) at KUCA, for the ADS experiments with 100 MeV protons (Pb-Bi target). Then, the high-energy neutrons caused by the neutron yield at the location of target were attained in the injection of 100 MeV protons onto these targets. Also kinetic parameters of prompt neutron decay constant and subcriticality were experimentally estimated, when the source neutron spectrum was varied by the kind of accelerator, such as 14 MeV neutrons or spallation neutrons (100 MeV protons with Pb-Bi target). The objective of this study was to investigate experimentally the neutron characteristics of EE1 core in the ADS experiments with 100 MeV protons, when the neutron spectrum in high-energy region and the neutron yield of high-energy neutrons were acquired with the use of the solid targets, through the static and kinetic experiments, and to evaluate the accuracy of the Monte Carlo analyses through the calculations by the MCNP6.1 code with JENDL-4.0 for transport, JENDL/HE-2007 for high-energy protons and neutrons, and JENDL/D-99 libraries for reaction rates.

1-2   Experimental Settings

1.2.1   Description of KUCA core

KUCA comprises solid-moderated and -reflected type-A and -B cores, and a water-moderated and -reflected type-C core. In the present series of experiments, the solid-moderated and -reflected type-A core was combined with a Cockcroft-Walton type pulsed neutron generator and the FFAG accelerator at KUCA.

The A-core (A1/8"p60EUEU(3)) configuration used for measuring the reaction rates is shown in Fig. 1-1. The fuel rods were constructed of a combination of 26 elements that were loaded on the grid plate. The materials used in the critical assemblies were always in the form of rectangular parallelepipe, 2" sq. with thickness ranging between 1/16" and 2". The upper and lower parts of the fuel region were polyethylene reflector layers of more than 500 mm long, as shown in Fig. 1-2. The fuel rod, a highly-enriched uranium-aluminum (U-Al) alloy, consisted of 60 cells of polyethylene plate 1/8" thick, and a U-Al plate 1/16" thick and 2" sq. The functional height of the core was approximately 400 mm.

1.2.2   Description of FFAG accelerator

100 MeV protons generated from the FFAG accelerator were injected onto the heavy metal target (Pb-Bi). The main characteristics are under the following parameters: 100 MeV energy, 1 nA intensity, 20 Hz pulsed frequency, 100 ns pulsed width and 40 mm diameter spot size at the target. The thickness of target was determined on the basis of previous analyses [18], [19] in the reaction rates for high-energy protons. A level of the neutron yield generated at the target was around 1.0×10^8 $1/s$ by an injection of 100 MeV protons onto the heavy metal target.

1-3 Experimental Results

1.3.1 Indium (In) reaction rate distribution

Indium (In) wire 1.0 mm diameter and 800 mm long was set in the axial center position along (17,16-L,Z) the vertical direction shown in Fig. 1-1 for measuring the reaction rate distribution. The experimental results of the In wire were obtained by measuring total counts of the peak energy of γ-ray emittance and normalized by the counts of irradiated In foil (10*10*1 mm) emitted from ^{115}In(n, n')^{115m}In (threshold energy 0.3 MeV) reactions set at the location of the target.

1.3.2 Time evolution data of PNS and Noise methods

To monitor carefully the prompt and delayed neutron behaviors, each core was set with three or four BF$_3$ detectors (1/2" and 1" diameters; 300 mm long) and optical fibers at the axial central positions, as shown in Fig. 1-1. Through the time evolution data of prompt and delayed neutrons, the prompt neutron decay constant was deduced by the least-square fitting of the time evolution of the neutrons to an exponential function over the time optimal duration. Subcriticality was deduced by the extrapolated area ratio method on the basis of the prompt and delayed neutron behaviors.

1.3.3 Critical position and Excess reactivity

The critical state was adjusted by maintaining the control rods in certain positions, and the excess reactivity was attained on the basis of its integral calibration curve obtained by the positive period method.

1-4 References

[1]   S. Shiroya, H. Unesaki, Y. Kawase, H. Moriyama and M. Inoue, "Accelerator Driven Subcritical System as a Future Neutron Source in Kyoto University Research Reactor Institute (KURRI) – Basic Study on Neutron Multiplication in the Accelerator Driven Subcritical Reactor," *Prog. Nucl. Energy*, **37**, 357 (2000).

[2]   S. Shiroya, A. Yamamoto, K. Shin, T. Ikeda, S. Nakano and H. Unesaki, "Basic Study on Accelerator Driven Subcritical Reactor in Kyoto University Research Reactor Institute (KURRI)," *Prog. Nucl. Energy*, **40**, 489 (2002).

[3]   C. H. Pyeon, Y. Hirano, T. Misawa, H. Unesaki, C. Ichihara, T. Iwasaki and S. Shiroya, "Preliminary Experiments on Accelerator Driven Subcritical Reactor with Pulsed Neutron Generator in Kyoto University Critical Assembly," *J. Nucl. Sci. Technol.,* **44**, 1368 (2007).

[4]   C. H. Pyeon, M. Hervault, T. Misawa, H. Unesaki, T. Iwasaki and S. Shiroya, "Static and Kinetic Experiments on Accelerator Driven Subcritical Reactor with 14 MeV Neutrons in Kyoto University Critical Assembly," *J. Nucl. Sci. Technol.,* **45**, 1171 (2008).

[5]   C. H. Pyeon, H. Shiga, T. Misawa, T. Iwasaki and S. Shiroya, "Reaction Rate Analyses for an Accelerator-Driven System with 14 MeV Neutrons in Kyoto University Critical Assembly," *J. Nucl. Sci. Technol.*, **46**, 965 (2009).

[6]   H. Shahbunder, C. H. Pyeon, T. Misawa and S. Shiroya, "Experimental Analysis for Neutron Multiplication by using Reaction Rate Distribution in Accelerator-Driven System," *Ann. Nucl. Energy*, **37**, 592 (2010).

[7]   H. Taninaka, K. Hashimoto, C. H. Pyeon, T. Sano, T. Misawa and T. Osawa, "Determination of Lambda-Mode Eigenvalue Separation of a Thermal Accelerator-Driven System from Pulsed Neutron Experiment," *J. Nucl. Sci. Technol.*, **47**, 376 (2010).

[8]   H. Shahbunder, C. H. Pyeon, T. Misawa, J. Y. Lim and S. Shiroya, "Subcritical Multiplication Factor and Source Efficiency in Accelerator-Driven System," *Ann. Nucl. Energy*, **37**, 1214 (2010).

[9]   H. Shahbunder, C. H. Pyeon, T. Misawa, J. Y. Lim and S. Shiroya, "Effects of Neutron Spectrum and External Neutron Source on Neutron Multiplication Parameters in Accelerator-Driven System," *Ann. Nucl. Energy*, **37**, 1785 (2010).

[10]   H. Taninaka, K. Hashimoto, C. H. Pyeon, T. Sano, T. Misawa, H. Unesaki, W. Sugiyama and T. Osawa, "Determination of Subcritical Reactivity of a Thermal Accelerator-Driven System from Beam Trip and Restart Experiment," *J. Nucl. Sci. Technol.*, **48**, 873 (2011).

[11]   H. Taninaka, A. Miyoshi, K. Hashimoto, C. H. Pyeon, T. Sano, T. Misawa, W. Sugiyama and T. Osawa, "Feynman-α Analysis for a Thermal Subcritical Reactor System Driven by an Unstable 14MeV-Neutron Source," *J. Nucl. Sci. Technol.*, **48**, 1272 (2011).

[12]   C. H. Pyeon, Y. Takemoto, T. Yagi, Y. Takahashi and T. Misawa, "Accuracy of Reaction Rates in the Accelerator-Driven System with 14 MeV Neutrons at the Kyoto University Critical Assembly," *Ann. Nucl. Energy*, **40**, 229 (2012).

[13]   A. Sakon, K. Hashimoto, W. Sugiyama, H. Taninaka, C. H. Pyeon, T. Sano, T. Misawa, H.

Unesaki and T. Ohsawa, "Power Spectral Analysis for a Thermal Subcritical Reactor System Driven by a Pulsed 14 MeV Neutron Source," *J. Nucl. Sci. Technol.*, **50**, 481 (2013).

[14] A. Sakon, K. Hashimoto, M. A. Maarof, M. Kawasaki, W. Sugiyama, C. H. Pyeon, T. Sano, T. Yagi and T. Ohsawa, "Measurement of Large Negative Reactivity of an Accelerator-Driven System in the Kyoto University Critical Assembly," *J. Nucl. Sci. Technol.,* **51**, 116 (2014).

[15] A. Sakon, K. Hashimoto, W. Sugiyama, S. Hohara, C. H. Pyeon, T. Sano, T. Yagi and T. Ohsawa, "Determination of Prompt-Neutron Decay Constant from Phase Shift between Beam Current and Neutron Detection Signals for an Accelerator-Driven System in the Kyoto University Critical Assembly," *J. Nucl. Sci. Technol.*, **52**, 204-213 (2015).

[16] T. Endo, A. Yamamoto, T. Yagi and C. H. Pyeon, "Statistical Error Estimation of the Feynman-α Method using the Bootstrap Method," *J. Nucl. Sci. Technol.*, **53**, 1447-1453 (2016).

[17] C. H. Pyeon, T. Misawa, J. Y. Lim *et al.*, "First Injection of Spallation Neutrons Generated by High-Energy Protons into the Kyoto University Critical Assembly," *J. Nucl. Sci. Technol.*, **46**, 1091 (2009).

[18] C. H. Pyeon, H. Shiga, K. Abe, H. Yashima, T. Nishio, T. Misawa, T. Iwasaki and S. Shiroya, "Reaction Rate Analysis of Nuclear Spallation Reactions Generated by 150, 190 and 235 MeV Protons," *J. Nucl. Sci. Technol.*, **47**, 1090 (2010).

[19] J. Y. Lim, C. H. Pyeon, T. Yagi and T. Misawa, "Subcritical Multiplication Parameters of the Accelerator-Driven System with 100 MeV Protons at the Kyoto University Critical Assembly," *Sci. Technol. Nucl. Install.*, **2012**, ID: 395878, 9 pages, (2012).

[20] Y. Takahashi, T. Azuma, T. Nishio, T. Yagi, C. H. Pyeon and T. Misawa, "Conceptual Design of Multi-Targets for Accelerator-Driven System Experiments with 100 MeV Protons," *Ann. Nucl. Energy*, **54**, 162 (2013).

[21] T. Yagi, C. H. Pyeon and T. Misawa, "Application of Wavelength Shifting Fiber to Subcriticality Measurements," *Appl. Radiat. Isot.*, **72**,11 (2013).

[22] C. H. Pyeon, T. Azuma, Y. Takemoto, T. Yagi and T. Misawa, "Experimental Analyses of External Neutron Source Generated by 100 MeV Protons at the Kyoto University Critical Assembly," *Nucl. Eng. Technol.*, **45**, 81 (2013).

[23] C. H. Pyeon, J. Y. Lim, Y. Takemoto, T. Yagi, T. Azuma, H. S. Kim, Y. Takahashi, T. Misawa and S. Shiroya, "Preliminary Study on the Thorium-Loaded Accelerator-Driven System with 100 MeV Protons at the Kyoto University Critical Assembly," *Ann. Nucl. Energy*, **38**, 2298 (2011).

[24] C. H. Pyeon, T. Yagi, K. Sukawa, Y. Yamaguchi and T. Misawa, "Mockup Experiments on the Thorium-Loaded Accelerator-Driven System in the Kyoto University Critical Assembly," *Nucl. Sci. Eng.*, **177**, 156-168 (2014).

[25] C. H. Pyeon, H. Nakano, M. Yamanaka, T. Yagi and T. Misawa, "Neutron Characteristics of Solid Targets in Accelerator-Driven System with 100 MeV Protons at Kyoto University Critical Assembly," *Nucl. Technol.*, **192**, 181-190 (2015).

[26] M. Yamanaka, C. H. Pyeon, T. Yagi and T. Misawa, "Accuracy of Reactor Physics Parameters in Thorium-Loaded Accelerator-Driven System Experiments at Kyoto University Critical Assembly," *Nucl. Sci. Eng.*, **183**, 96-106 (2016).

[27] J. B. Lagrange, T. Planche, E. Yamakawa *et al.*, "Straight Scaling FFAG Beam Line," *Nucl. Instrum. Methods A*, **691**, 55 (2013).

[28] E. Yamakawa, T. Uesugi, J. B. Lagrange *et al.*, "Serpentine Acceleration in Zero-Chromatic FFAG Accelerators," *Nucl. Instrum. Methods A*, **716**, 46 (2013).

Appendix-I
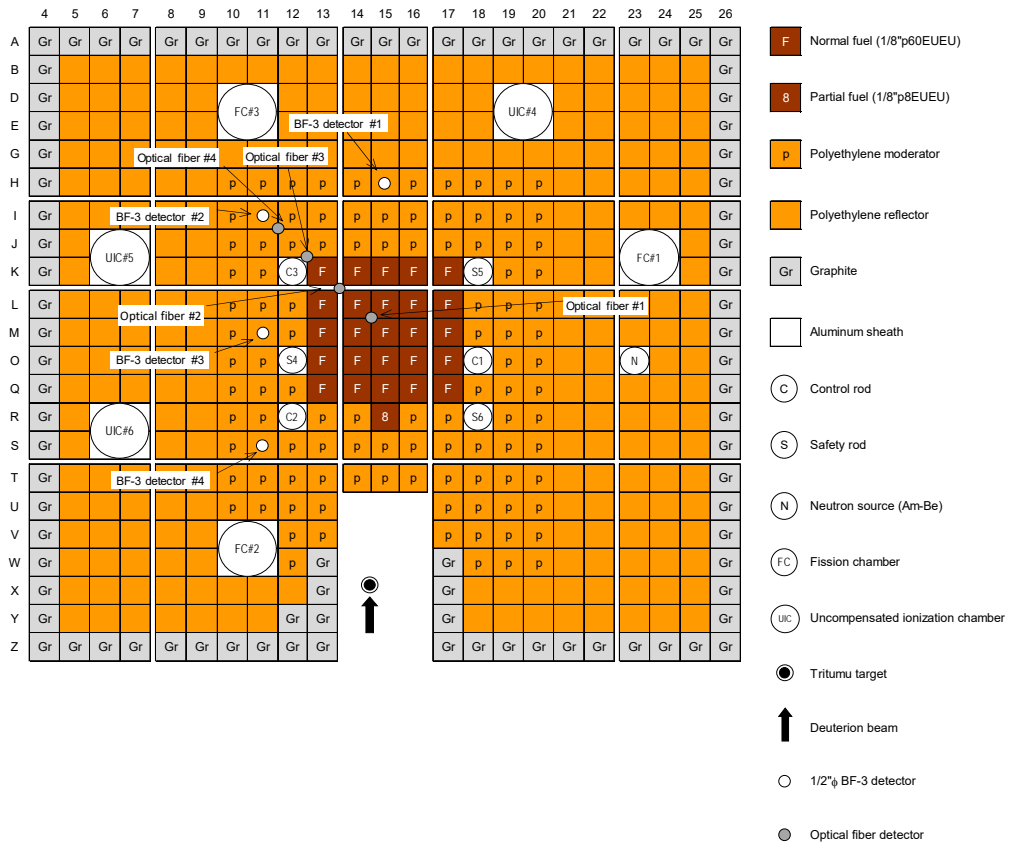
Fig. 1-1   The general view of KUCA core configuration
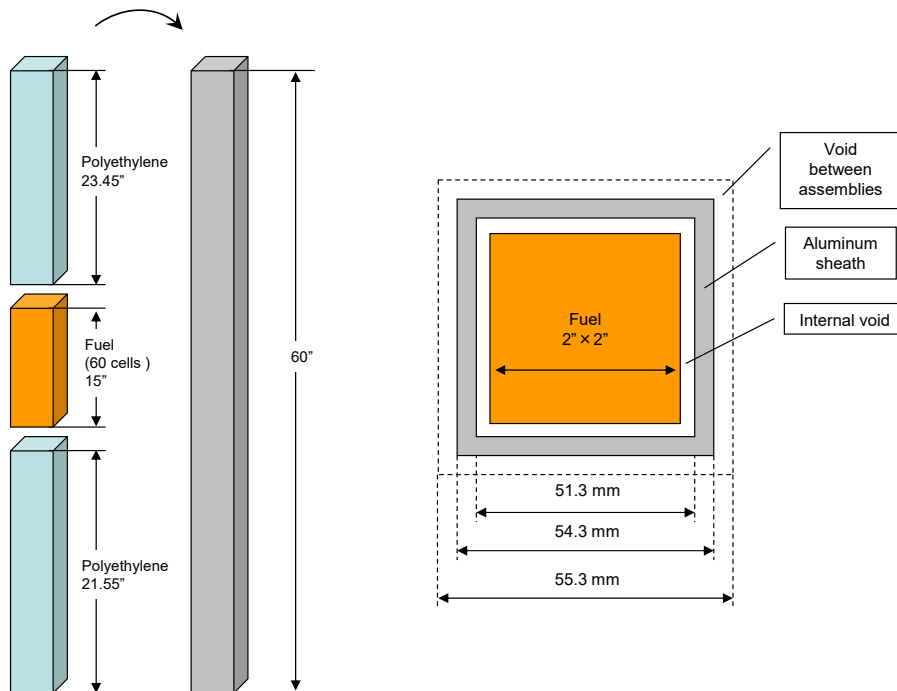
Fig. 1-2   Description of fuel assembly at KUCA

Fig. 1-3　Description of fuel (HEU; 2"×2") and polyethylene plates (2"×2")
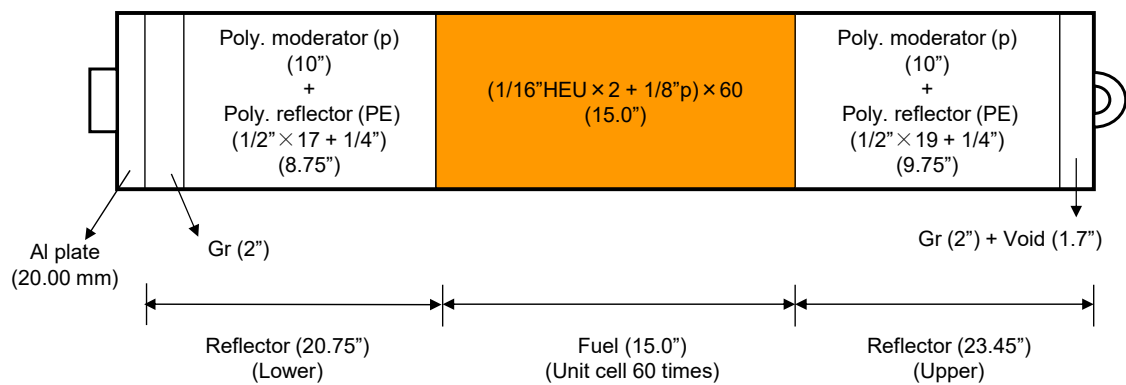
Fig. 1-4　Fall sideways view of fuel assembly "F" shown in Fig. 1-1

1/16"HEU = 1.5875 mm
1/8"p = 3.158 mm
10"p = 254.00 mm
1/4"PE = 6.300 mm
1/2"PE = 12.500 mm
2"Gr = 50.80 mm
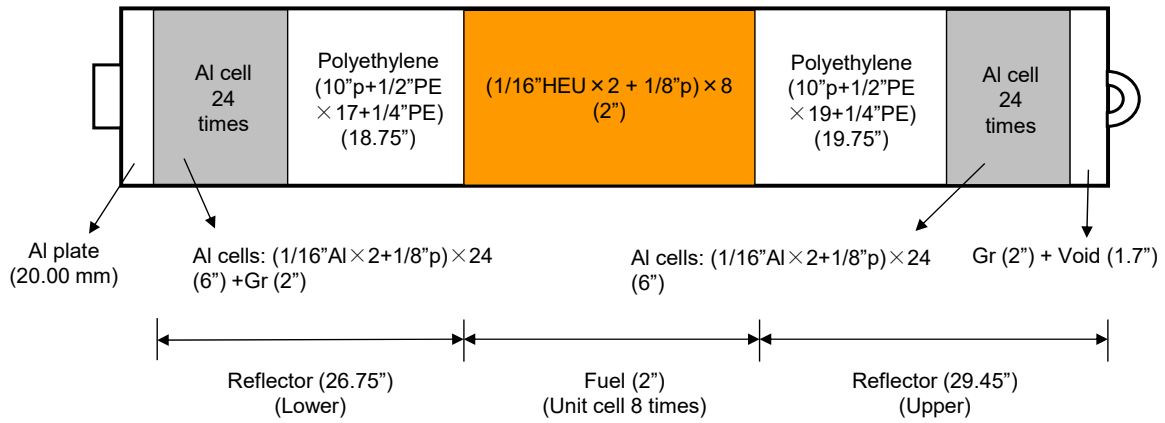
(a) Partial fuel assembly "8"
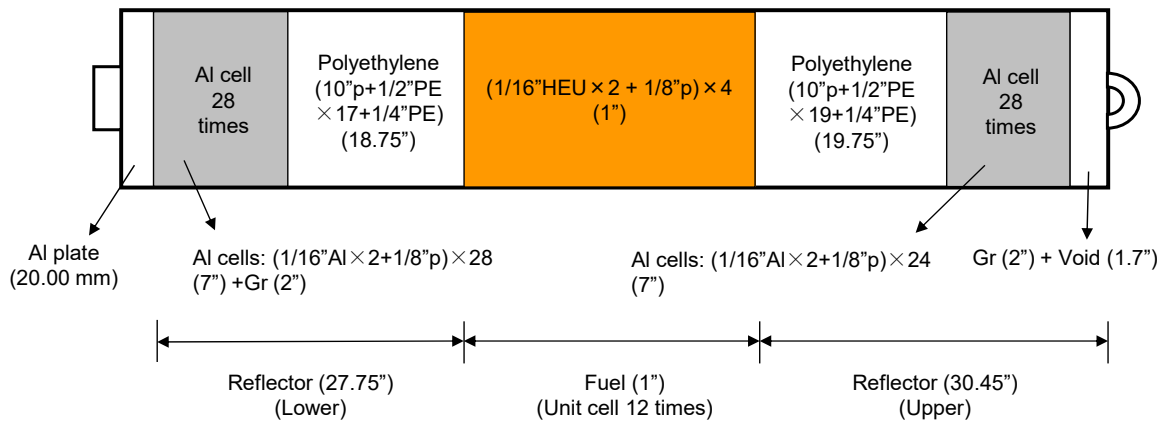
(b) Partial fuel assembly "4"

Fig. 1-5   Fall sideways view of fuel assembly "8" shown in Fig. 1-1

1/16"Al = 1.5875 mm
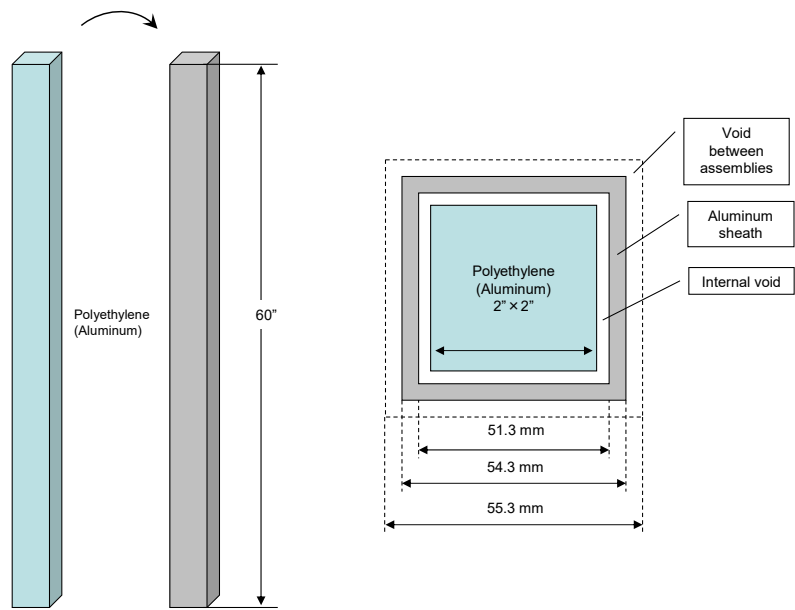
Fig. 1-5   Description of polyethylene reflector at KUCA
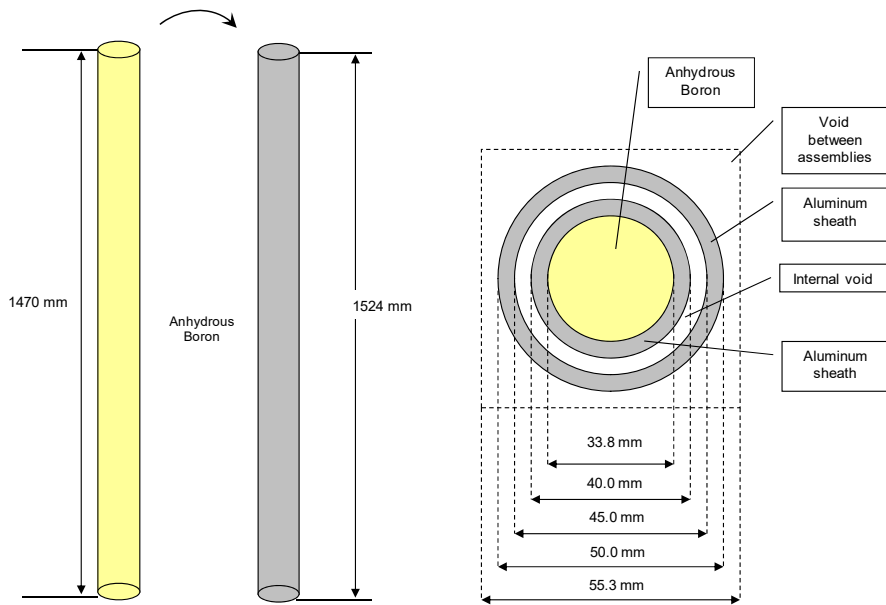
Fig. 1-6   Description of control (safety) rod at KUCA
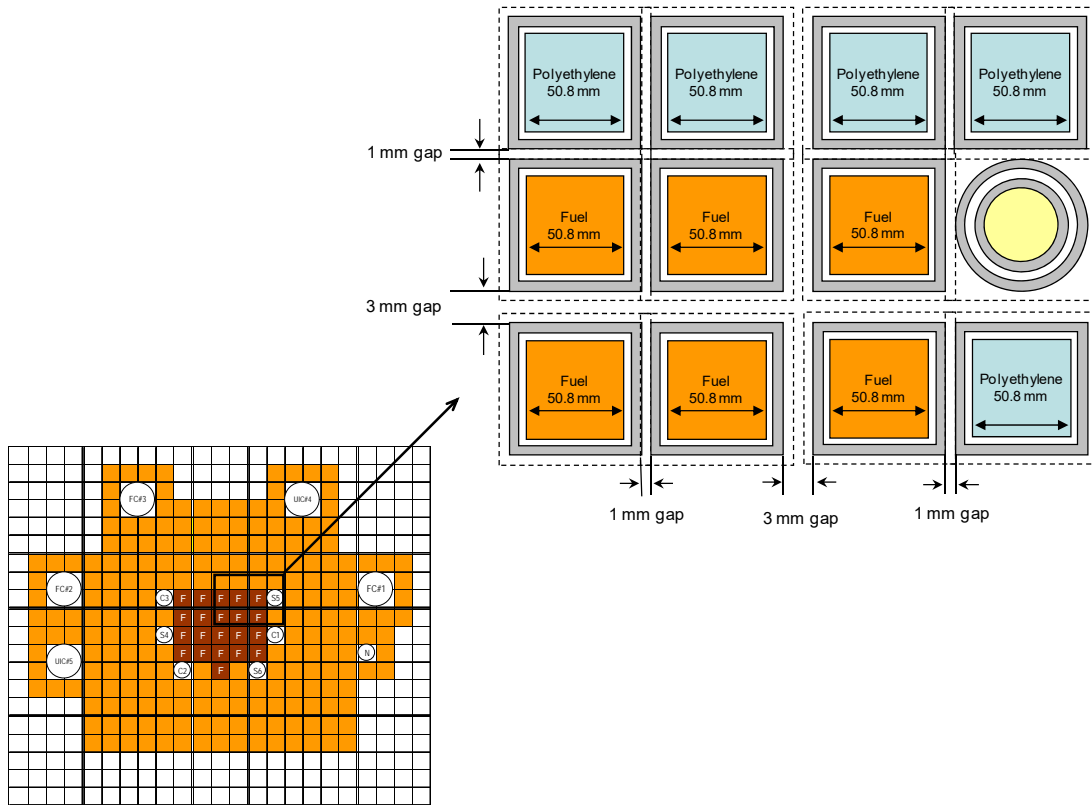
Fig. 1-7   Description of fuel assembly, polyethylene reflector and control rod at KUCA
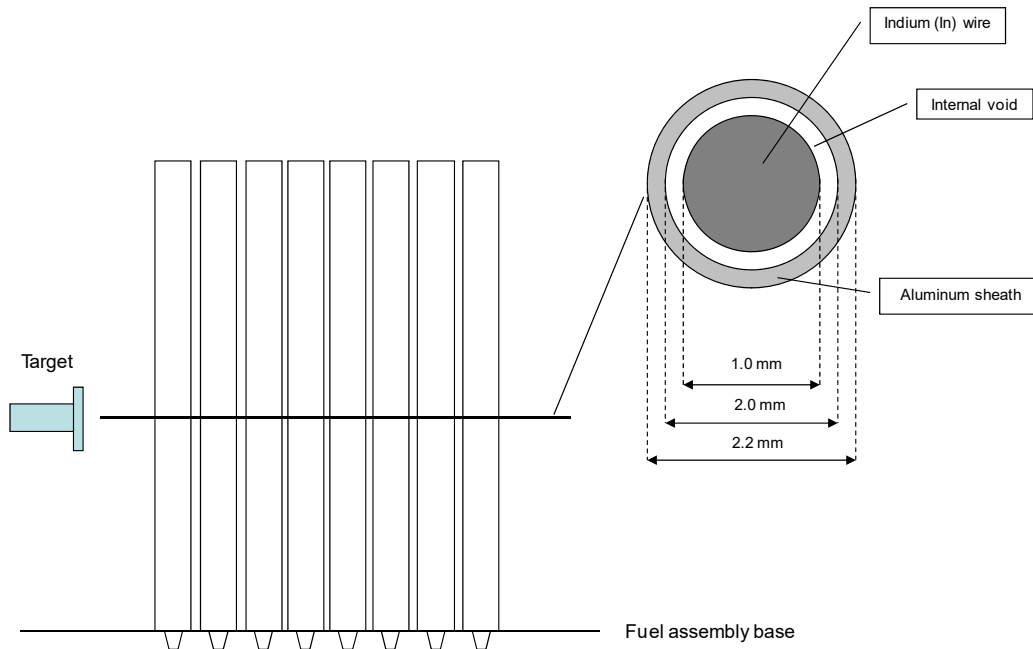
Fig. 1-8   Setting of Indium (In) wire
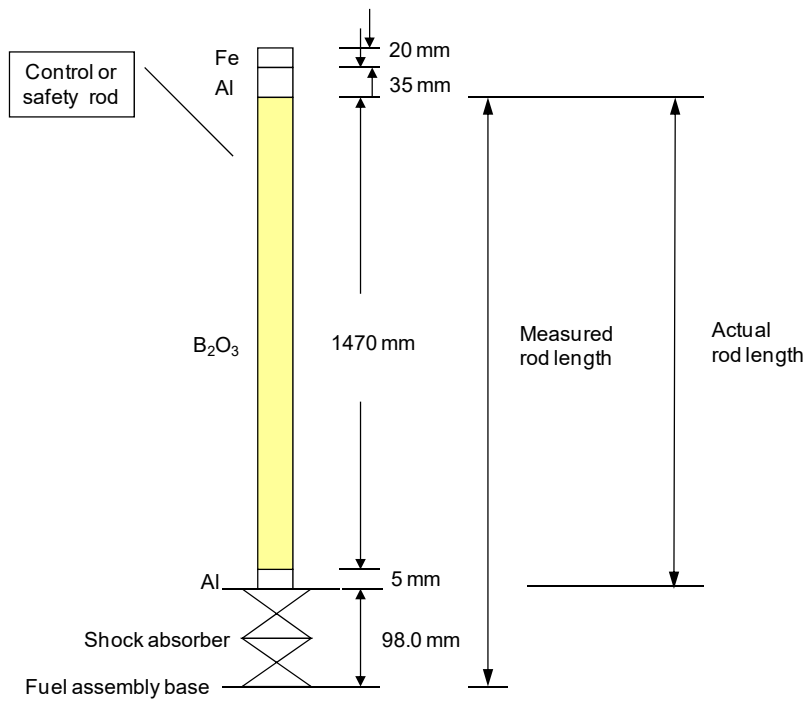
Fig. 1-9   Actual position of control (safety) rod
(Actual position = Measured position – 97.5 mm)

Thickness (x)
W: 12 mm
W-Be: 12 mm – 10 mm (in Be and W order for proton beams)
Pb-Bi: 18 mm

Al foli (10*10*1 mm)
Target (50 mm diam., x mm thick)
In foil (10*10*1 mm)
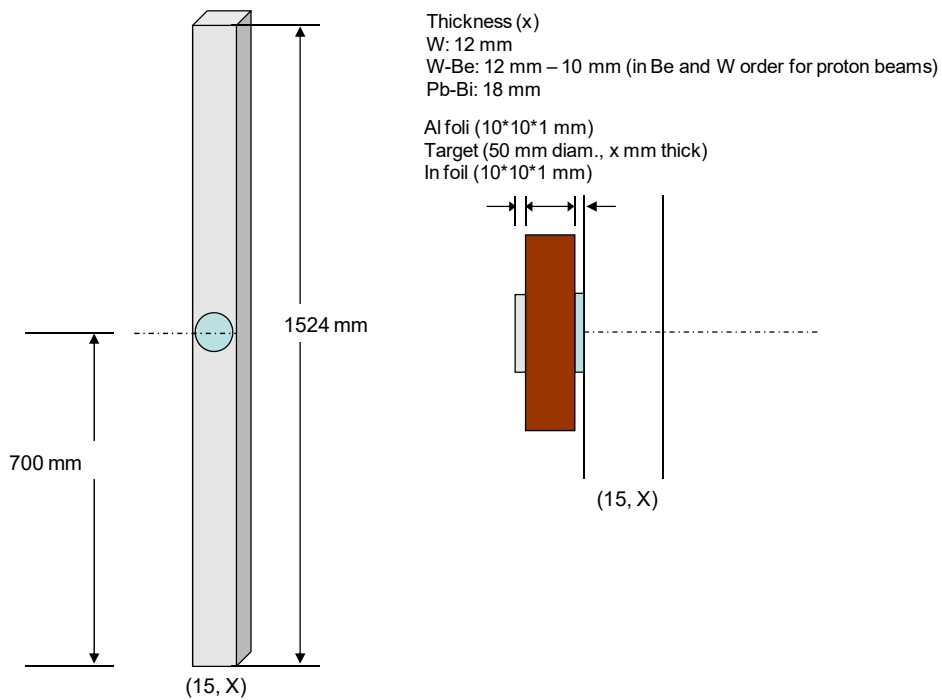
Fig. 1-10   Attachment of target, Al and In foils at the location of core target
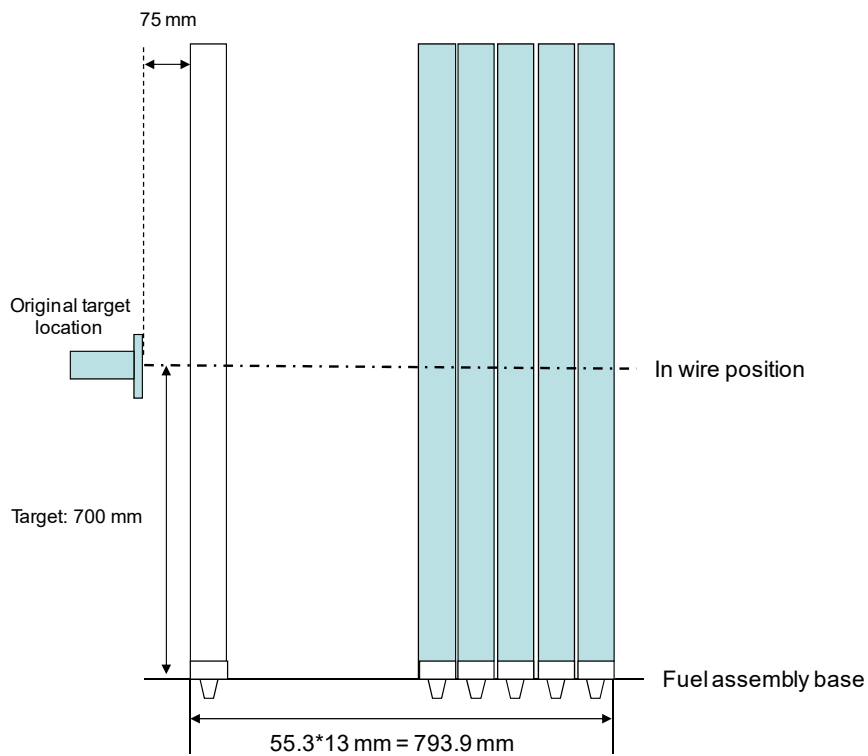
Fig. 1-11　Side view of target and core configuration with 100 MeV protons
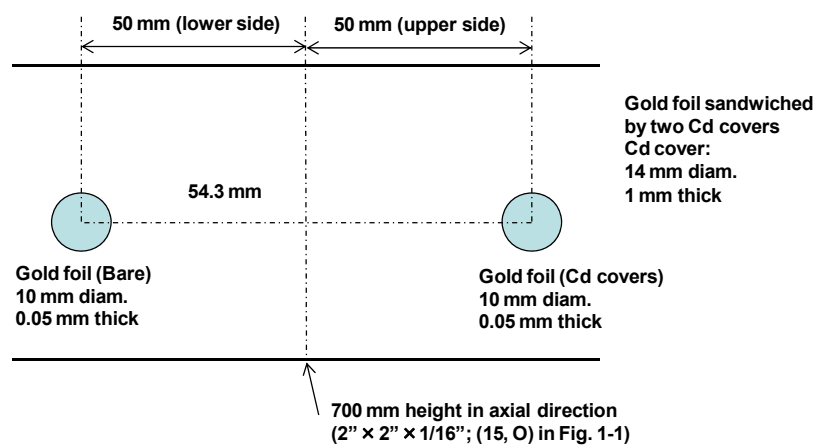
Fig. 1-12　Fall sideways view of HEU fuel rod in (15, O; Fig. 1-1)

80 mm

3 mm

48 mm

100 mm

3 mm

50 mm

Proton beams (40 mm diameter)

Enlarged (flange; Original target location)

1 mm

3 mm

10 mm

50 mm

10 mm

50 mm
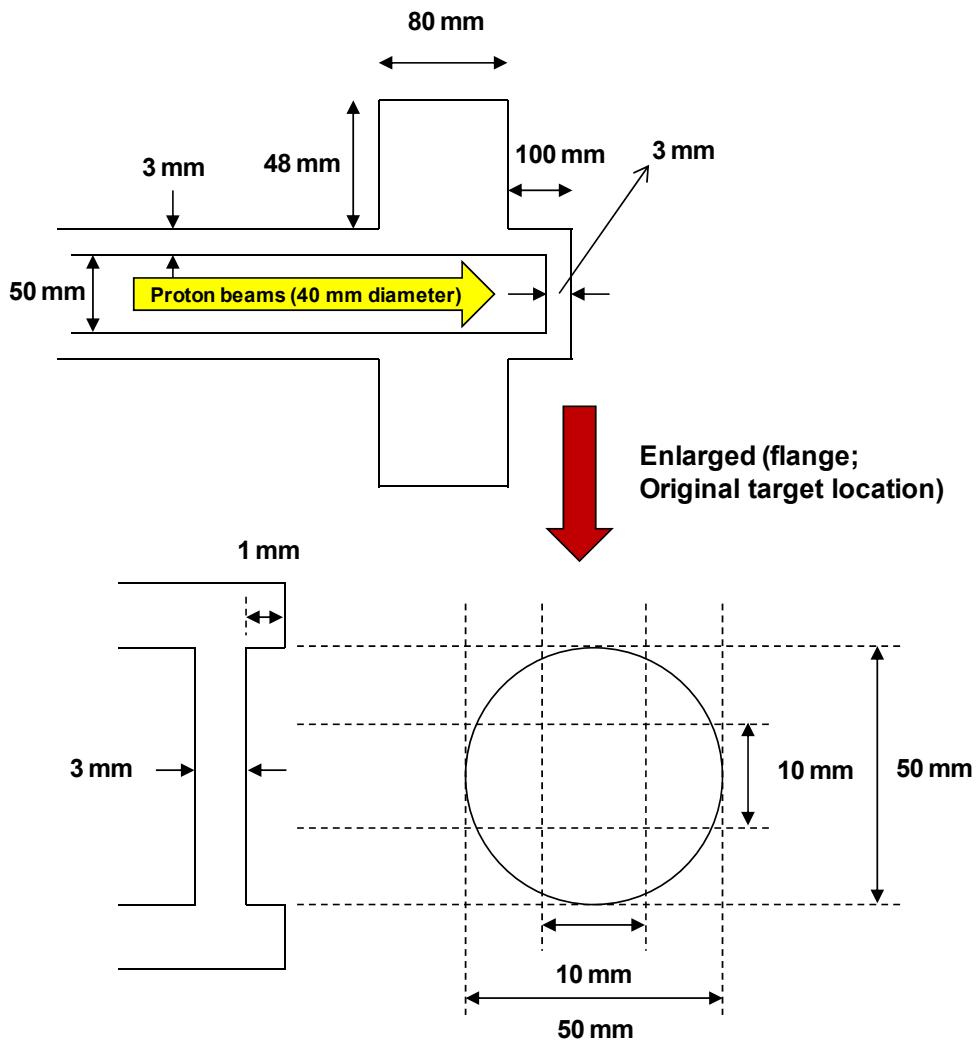
Fig. 1-13   Target configuration of the location of original target

Table 1-1　Atomic densities of 1/16" thick highly-enriched uranium (HEU) fuel plate (U-Al alloy)

Isotope	Atomic density [×10²⁴/cm³] (1/16"HEU = 1.5875 mm)
^{234}U	1.13659E-05
^{235}U	1.50682E-03
^{236}U	4.82971E-06
^{238}U	9.25879E-05
Al	5.56436E-02

Table 1-2　Atomic densities of polyethylene (PE) reflector

Isotope	Atomic density [×10²⁴/cm³]			
	1/2"PE thick plate (12.500 mm)	1/4"PE thick plate (6.300 mm)	1/8"PE thick plate (3.086 mm)	19"PE Polyethylene square rod (483.085 mm)
H	8.06560E-02	8.08711E-02	8.02167E-02	8.00083E-02
C	4.03280E-02	4.04356E-02	4.01084E-02	4.00042E-02

Table 1-3　Atomic density of polyethylene moderator "p" shown in Figs. 1-4 and 1-5

Isotope	Atomic density [×10²⁴/cm³]	
	1/8"p thick plate (3.158 mm)	10"p Polyethylene square rod (254.00 mm)
H	7.77938E-02	7.97990E-02
C	3.95860E-02	4.08960E-02

Table 1-4   Atomic densities of control and safety rods

Isotope	Atomic density [$\times 10^{24}$/cm^3]
^{10}B	3.87448E-03
^{11}B	1.68447E-02
^{16}O	3.10787E-02

Table 1-5   Atomic density of aluminum sheath and 1/16"Al plate for the core element

Isotope	Atomic density [$\times 10^{24}$/cm^3] (1/16"Al = 1.5875 mm)
Al	6.00385E-02

Table 1-6   Atomic density of 2"Gr plate for the core element

Isotope	Atomic density [$\times 10^{24}$/cm^3] (2"Gr = 50.80 mm)
C	8.64182E-02

Table 1-7   Atomic densities of Cd, In and Au

Foil (Wire)	Isotope	Abundance (%)	Purity (%)	Atomic density [$\times 10^{24}$/cm^3]
Cd	^{106}Cd	1.25	99.99	5.39648E-04
	^{108}Cd	0.89	99.99	3.91477E-04
	^{110}Cd	12.51	99.99	5.59564E-03
	^{111}Cd	12.81	99.99	5.78677E-02
	^{112}Cd	24.13	99.99	1.10072E-02
	^{113}Cd	12.22	99.99	5.62419E-03
	^{114}Cd	28.72	99.99	1.33398E-02
	^{116}Cd	7.47	99.99	3.53884E-03
In	^{113}In	4.29	99.99	1.64406E-03
	^{115}In	95.71	99.99	3.66790E-02
Au	^{197}Au	100	99.95	5.90403E-02

Table 1-8   Atomic densities of W, Be and Pb-Bi

Target	Isotope	Abundance (%)	Atomic density [$\times 10^{24}$/cm^3]
Pb-Bi (44.5/55.5)	^{204}Pb	1.4	1.87461E-04
	^{206}Pb	24.1	3.25860E-03
	^{207}Pb	22.1	3.00266E-03
	^{208}Pb	52.4	7.15378E-03
	^{209}Bi	100	1.67670E-02

Table 1-9　　Dimension of target

Target	Diameter [mm]	Thickness [mm]
Pb-Bi	50.0	18.0

Table 1-10　　Atomic densities of beam tube component (SUS304) shown in Fig. 1-13

Isotope	Atomic density [$\times 10^{24}$/cm^3]
^{54}Fe	3.55712E-03
^{56}Fe	5.58391E-02
^{57}Fe	1.28957E-03
^{58}Fe	1.71618E-04
^{50}Cr	7.51530E-04
^{52}Cr	1.44925E-02
^{53}Cr	1.64333E-03
^{54}Cr	4.09060E-04
^{58}Ni	5.10587E-03
^{60}Ni	1.96674E-03
^{61}Ni	8.54932E-05
^{62}Ni	2.72597E-04
^{64}Ni	6.94130E-05

2. Core Configurations

2-1 ADS with 14 MeV neutrons
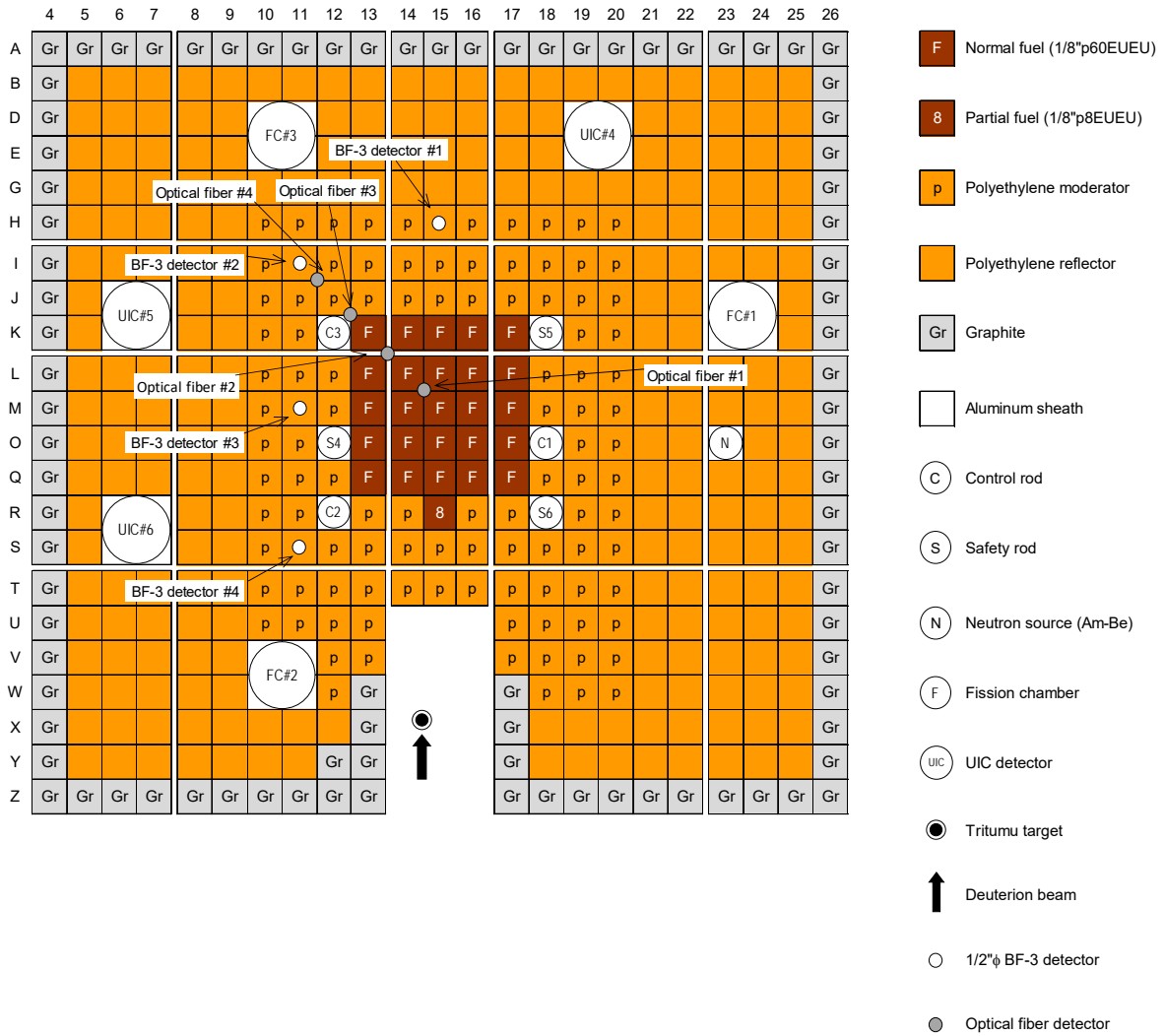
Fig. 2-1 Core configuration (EE1 core) of ADS with 14 MeV neutrons
(Case 1-D: Critical core; 3016 HEU plates)
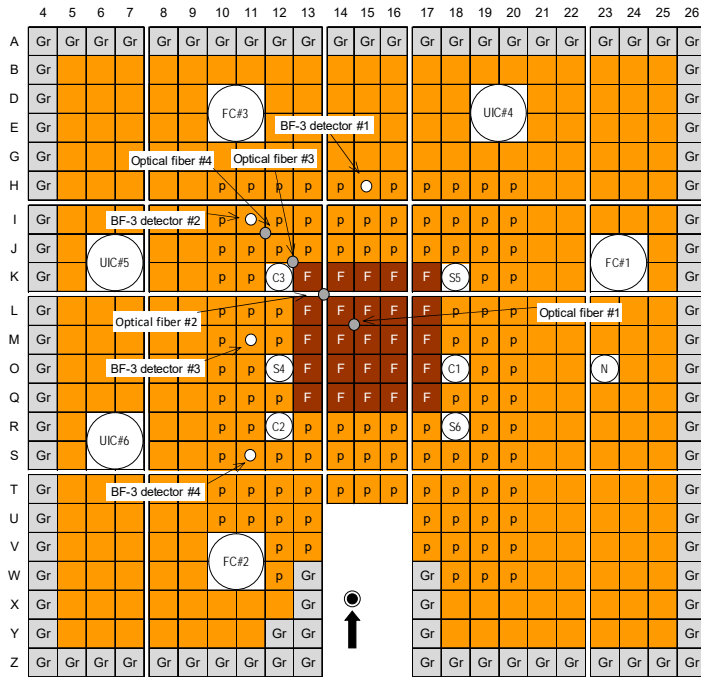
(a) Case 2-D (3000 HEU plates)

(b) Case 3-D (2760 HEU plates)

(c) Case 4-D (2520 HEU plates)
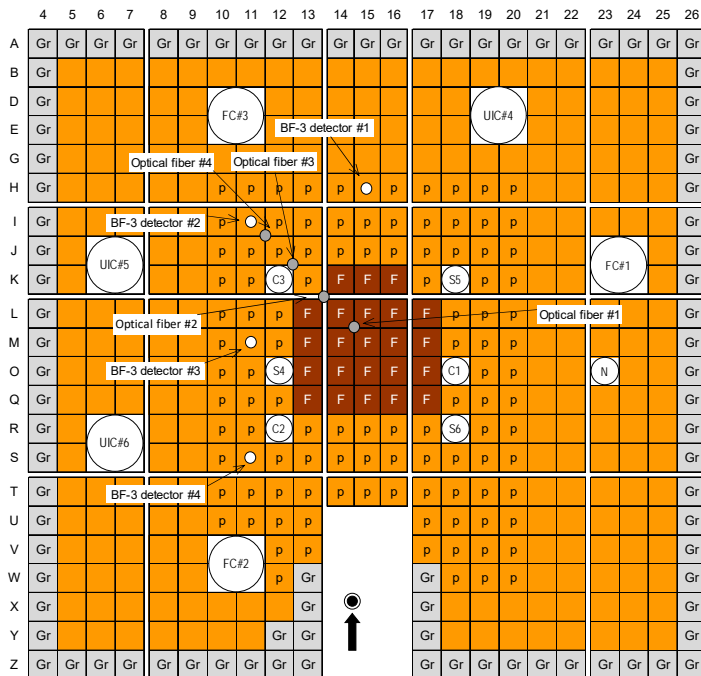
(d) Case 5-D (2280 HEU plates)
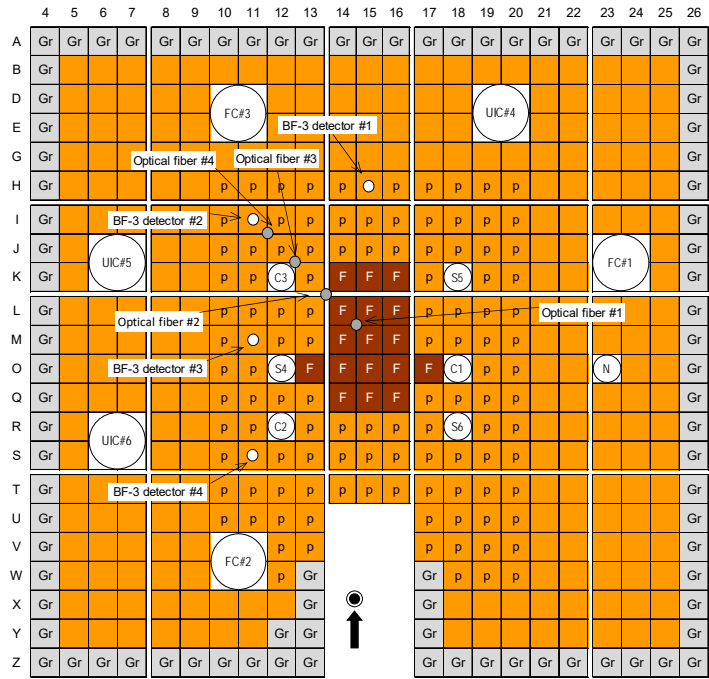
(e) Case 6-D (2040 HEU plates)

Fig. 2-2 Core configuration (EE1 core) of ADS with 14 MeV neutrons (Subcritical cores)

2-2　ADS with 100 MeV protons
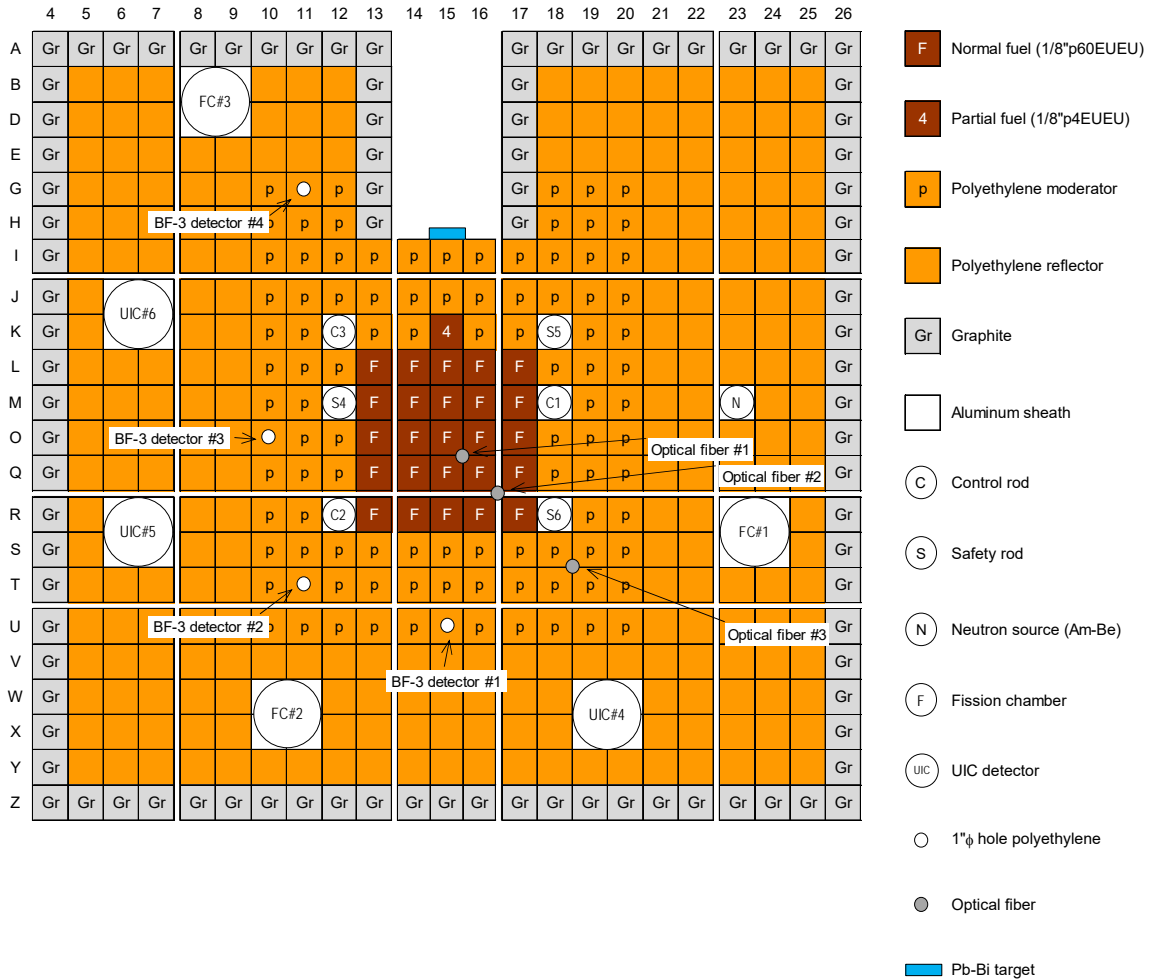
Fig. 2-3　Core configuration (EE1 core) of ADS with 100 MeV protons
(Case 1-F: Critical core; 3008 HEU plates)
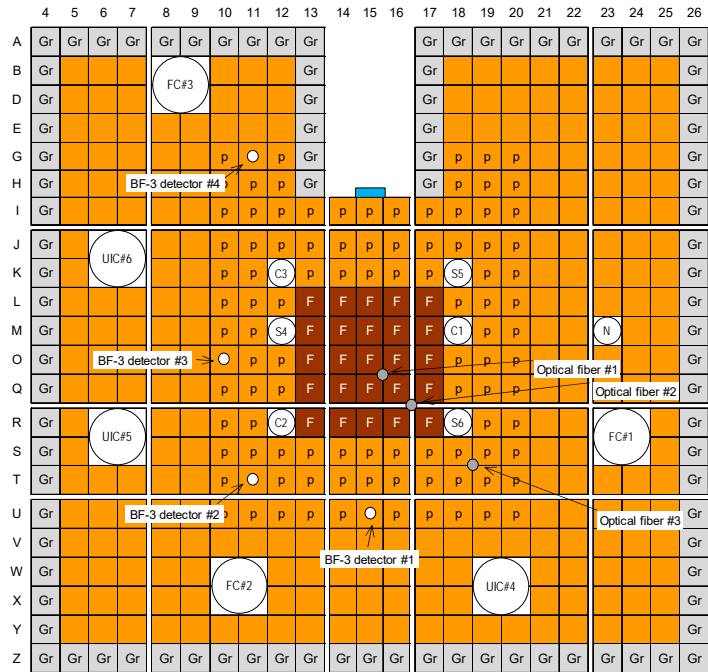
(a) Case 2-F (3000 HEU plates)
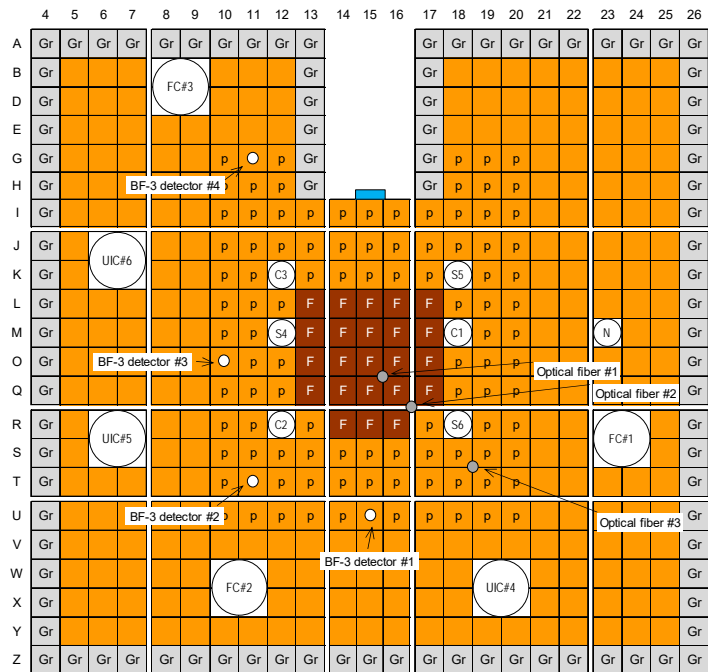
(b) Case 3-F (2760 HEU plates)
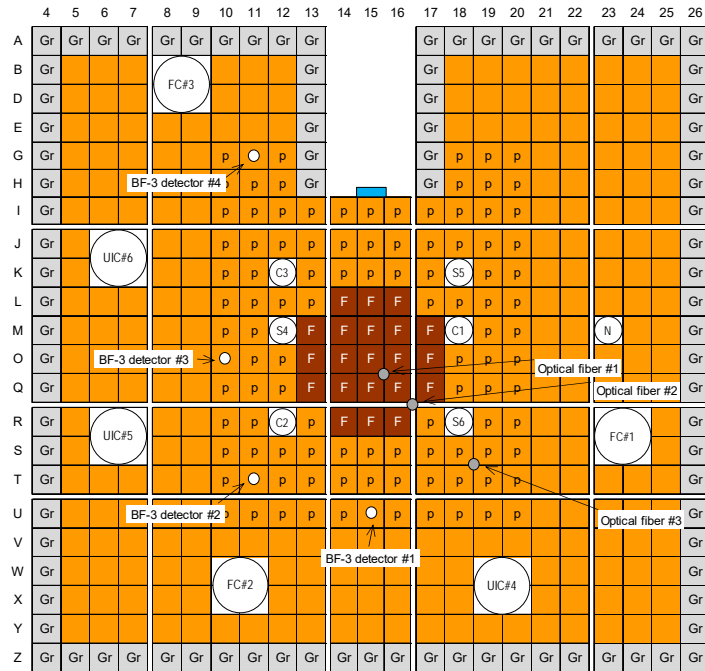
(c) Case 4-F (2520 HEU plates)
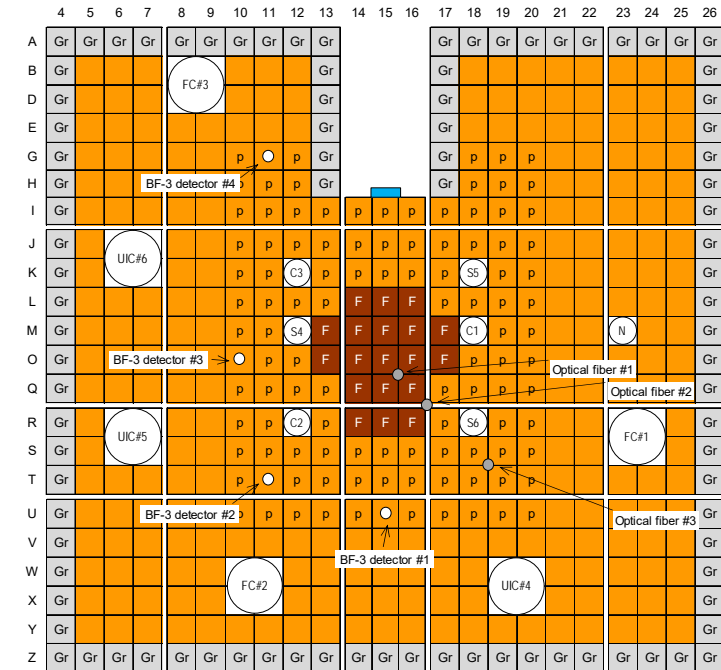
(d) Case 5-F (2280 HEU plates)
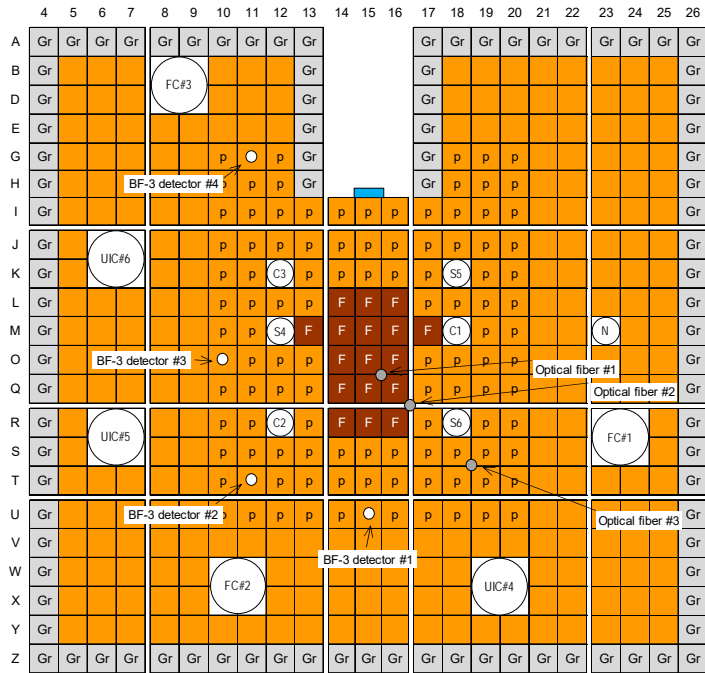
(e) Case 6-F (2040 HEU plates)

Fig. 2-4　Core configuration (EE1 core) of ADS with 100 MeV protons (Subcritical cores)

3.   Results of Experiments

3-1   Criticality and Control rod worth

Table 3-1   Control rod positions at the critical state (Case 1-D)

Rod	Rod position [mm]
C1	1200.00
C2	1200.00
C3	630.01
S4	1200.00
S5	1200.00
S6	1200.00
Excess reactivity [pcm]	271.7 ± 1.0

Table 3-2   Control rod worth (Case 1-D)

Rod	Rod worth [pcm]
C1 (S4)	867.4 ± 3.9
C2 (S6)	142.8 ± 3.5
C3 (S5)	506.4 ± 41.3

Table 3-3　Control rod positions at the critical state (Case 1-F) (2019.01.29)

Rod	Rod position [mm]
C1	1200.00
C2	723.31
C3	1200.00
S4	1200.00
S5	1200.00
S6	1200.00
Excess reactivity [pcm]	102.5 ± 1.8

Table 3-4　Control rod worth (Case 1-F)

Rod	Rod worth [pcm]
C1 (S4)	866.7 ± 20.7
C2 (S6)	439.4 ± 31.9
C3 (S5)	148.6 ± 7.6

3.2　Time evolution data of PNS and Noise methods

Table 3-5　List of core condition in all the cores shown in Fig. 2-1

Case	Number of fuel plates	Rod insertion (down)	14 MeV neutrons		
			Repetition [Hz]	Width [μs]	Current [mA]
Case 1-D-1	3016	C1, C2, C3	100	97	0.12
Case 1-D-1T	3016	C1, C2, C3	100	97	0.12
Case 1-D-2	3016	C1, C2, C3	Am-Be		
Case 1-D-3	3016	C1, C2, C3	20	97	0.12
Case 1-D-4	3016	C1, C2, C3	20	97	0.12

Table 3-6　List of core condition in all the cores shown in Fig. 2-2(a)

Case	Number of fuel plates	Rod	14 MeV neutrons		
			Repetition [Hz]	Width [μs]	Current [mA]
Case 2-D-1	3000	C1~S6 up	20	97	0.12
Case 2-D-2	3000	C1 down	20	97	0.12
Case 2-D-3	3000	C1 down	50	97	0.12

Table 3-7　List of core condition in all the cores shown in Fig. 2-2(b)

Case	Number of fuel plates	Rod	14 MeV neutrons		
			Repetition [Hz]	Width [μs]	Current [mA]
Case 3-D-1	2760	C1~S6 up	20	97	0.12

Table 3-8 List of core condition in all the cores shown in Fig. 2-2(c)

Case	Number of fuel plates	Rod	14 MeV neutrons		
			Repetition [Hz]	Width [μs]	Current [mA]
Case 4-D-1	2520	C1~S6 up	20	85	0.08
Case 4-D-1T	2520	C1~S6 up	50	85	0.08
Case 4-D-2	2520	C1~S6 up	50	85	0.08
Case 4-D-3	2520	C1~S6 up	20	75	0.15
Case 4-D-4T	2520	C1~S6 up	50	85	0.15
Case 4-D-5	2520	C1~S6 up	50	85	0.15

Table 3-9 List of core condition in all the cores shown in Fig. 2-2(d)

Case	Number of fuel plates	Rod	14 MeV neutrons		
			Repetition [Hz]	Width [μs]	Current [mA]
Case 5-D-1	2280	C1~S6 up	20	97	0.08
Case 5-D-2	2280	C1~S6 up	100	97	0.08
Case 5-D-3T	2280	C1~S6 up	20	97	0.08
Case 5-D-3	2280	C1~S6 up	20	97	0.08
Case 5-D-4	2280	C1~S6 up	50	97	0.08

Table 3-10 List of core condition in all the cores shown in Fig. 2-2(e)

Case	Number of fuel plates	Rod	14 MeV neutrons		
			Repetition [Hz]	Width [μs]	Current [mA]
Case 6-D-1T	2040	C1~S6 up	20	93	0.10
Case 6-D-2	2040	C1~S6 up	100	97	0.10
Case 6-D-3	2040	C1~S6 up	50	97	0.08
Case 6-D-4T	2040	C1~S6 up	50	97	0.08
Case 6-D-5	2040	C1~S6 up	500	20	0.2

Table 3-11　List of core condition in all the cores shown in Fig. 2-3

Case	Number of fuel plates	Rod insertion (down)	100 MeV protons		
			Repetition [Hz]	Width [ns]	Current [nA]
Case 1-F-1	3008	C1, C2, C3	30	100	0.4
Case 1-F-2	3008	C1, C2, C3	30	100	0.4
Case 1-F-3	3008	C1, C2, C3, S4	30	100	0.4
Case 1-F-4	3008	C1~S6	30	100	0.4
Case 1-F-5	3008	C1~S6, CC	30	100	0.4

CC: Center core

Transient steps:　　All C1~S6 up (stable)

　　　　　　　　　-> C1~C3 drop

　　　　　　　　　-> S4 drop

　　　　　　　　　-> S5 and S6 drop

　　　　　　　　　-> Center core drop

No data on Case 2-F

Table 3-12　List of core condition in all the cores shown in Fig. 2-4(c)

Case	Number of fuel plates	Rod insertion (down)	100 MeV protons		
			Repetition [Hz]	Width [ns]	Current [nA]
Case 3-F-1	2760	C1~S6 up	30	100	0.3
Case 3-F-2	2760	C1	30	100	0.3
Case 3-F-3	2760	C1, C2	30	100	0.3
Case 3-F-4	2760	C1, C2, C3	30	100	0.3
Case 3-F-5	2760	C1~S6, CC	30	100	0.3

CC: Center core

Transient steps:　All C1~S6 up (stable)

　　　　　　　　-> C1 drop

　　　　　　　　-> C2 drop

　　　　　　　　-> C3 drop

　　　　　　　　-> CC drop

Table 3-13　List of core condition in all the cores shown in Fig. 2-4(d)

Case	Number of fuel plates	Rod insertion (down)	100 MeV protons		
			Repetition [Hz]	Width [ns]	Current [nA]
Case 4-F-1	2520	C1~S6 up	30	100	0.3
Case 4-F-2	2520	C1	30	100	0.3
Case 4-F-3	2520	C1, C2	30	100	0.3
Case 4-F-4	2520	C1, C2, C3	30	100	0.3
Case 4-F-5	2520	C1~S6, CC	30	100	0.3

CC: Center core

Transient steps:　　All C1~S6 up (stable)

　　　　　　　　　-> C1 drop
　　　　　　　　　-> C2 drop
　　　　　　　　　-> C3 drop
　　　　　　　　　-> CC drop
　　　　　　　　　-> CC drop

Table 3-14　List of core condition in all the cores shown in Fig. 2-4(e)

Case	Number of fuel plates	Rod insertion (down)	14 MeV neutrons		
			Repetition [Hz]	Width [ns]	Current [nA]
Case 5-F-1	2280	C1~S6 up	30	100	0.3
Case 5-F-2	2280	C1	30	100	0.3
Case 5-F-3	2280	C1, C2	30	100	0.3
Case 5-F-4	2280	C1, C2, C3	30	100	0.3
Case 5-F-5	2280	C1~S6, CC	30	100	0.3

CC: Center core

Transient steps:　All C1~S6 up (stable)

　　　　　　　-> C1 drop

　　　　　　　-> C2 drop

　　　　　　　-> C3 drop

　　　　　　　-> CC drop

4. Kinetics Parameters

4.1 14 MeV Neutrons

Table 4-1-1 Measured prompt neutron decay constants α [1/s] deduced by PNS and Feynman-α methods

Case 1-D-1 (DT acc.) ($\rho_{pcm, exp}$ = 1245.0±41.7 [pcm])				
Detector	PNS method	Feynman-α method	Area$\rho_\$$[$]	Extended area $\rho_\$$[$]
BF-3 #1	717.63 ± 12.28	650.92 ± 55.23	1.50189 ± 0.02694	1.79660 ± 0.04535
BF-3 #2	710.94 ± 13.02	729.76 ± 60.58	1.56681 ± 0.02954	1.76655 ± 0.04770
BF-3 #3	709.12 ± 4.96	725.23 ± 50.43	1.54026 ± 0.01131	1.62362 ± 0.01756
BF-3 #4	739.00 ± 23.75	1226.41 ± 53.52	2.36997 ± 0.03507	1.50892 ± 0.05004
Fiber #1	713.88 ± 23.23	-	1.42923 ± 0.04583	1.35279 ± 0.06973
Fiber #2	733.90 ± 11.74	-	1.38885 ± 0.02078	1.47719 ± 0.03464
Fiber #3	711.48 ± 11.43	-	1.56890 ± 0.02685	1.75388 ± 0.04286

Table 4-1-2 Measured prompt neutron decay constants α [1/s] deduced by PNS and Feynman-α methods

Case 1-D-2 (Am-Be) ($\rho_{pcm, exp}$ =1245.0±41.7 [pcm])		
Detector	PNS method	Feynman-α method
BF-3 #1	-	745.76 ± 154.62
BF-3 #2	-	1051.355 ± 265.21
BF-3 #3	787.35 ± 68.45	604.28 ± 27.36
BF-3 #4	-	1057.10 ± 245.31
Fiber #1	-	865.09 ± 1492.43
Fiber #2	-	1179.31 ± 288.01
Fiber #3	-	645.96 ± 113.23

Table 4-1-3　　Measured prompt neutron decay constants α [1/s] deduced by PNS and Feynman-α methods

Case 1-D-3 (DT acc.) ($\rho_{pcm, exp}$ = 1245.0±41.7 [pcm])		
Detector	PNS method	Feynman-α method
BF-3 #1	-	-
BF-3 #2	-	-
BF-3 #3	715.18 ± 9.57	744.54 ± 8.70
Fiber #1	-	-
Fiber #2	724.51 ± 24.58	843.73 ± 139.74
Fiber #3	740.00 ± 26.794	977.05 ± 196.02

Table 4-1-4　　Measured prompt neutron decay constants α [1/s] deduced by PNS and Feynman-α methods

Case 1-D-4 (DT acc.) ($\rho_{pcm, exp}$ = 1245.0±41.7 [pcm])		
Detector	PNS method	Feynman-α method
BF-3 #1	-	-
BF-3 #2	-	-
BF-3 #3	713.43 ± 2.80	708.85 ± 3.28
Fiber #1	-	-
Fiber #2	715.59 ± 6.03	730.10 ± 5.92
Fiber #3	705.76 ± 6.19	728.07 ± 6.86

Table 4-1-5　Measured prompt neutron decay constants α [1/s] deduced by PNS and Feynman-α methods, $\rho_\$$ in dollar units by the area ratio method, and βeff/Λ (1/s) by the α-fitting method

	Case 2-D-1 (DT acc.) ($\rho_{pcm, MCNP}$ = 70.2 ± 5.7 [pcm])			
Detector	α (PNS method)	α (Feynman-α method)	Extended area $\rho_\$$ [$]	β_{eff}/Λ [1/s]
BF-3 #1	294.78 ± 29.27	319.16 ± 71.63	0.02283 ± 0.00703	288.2 ± 93.3
BF-3 #2	226.96 ± 23.31	363.98 ± 75.69	0.01576 ± 0.00537	223.4 ± 79.5
BF-3 #3	258.58 ± 12.34	270.42 ± 13.87	0.01938 ± 0.00270	253.7 ± 37.3
Fiber #1	248.38 ± 39.04	-	0.02066 ± 0.00559	243.4 ± 72.1
Fiber #2	229.95 ± 14.51	268.82 ± 20.68	0.01998 ± 0.00320	225.4 ± 38.8
Fiber #3	273.99 ± 26.24	310.39 ± 42.98	0.02613 ± 0.00559	267.0 ± 62.6

MCNP6.1 with ENDF/B-VII.0: β_{eff} = 829.0 [pcm], Λ = 3.147E-05 [s], β_{eff} / Λ = 263.43 [s]

Table 4-1-6　Measured prompt neutron decay constants α [1/s] deduced by PNS and Feynman-α methods

	Case 2-D-2 (DT acc.) ($\rho_{pcm, exp}$ = 855.7±41.34 [pcm])			
Detector	PNS method	Feynman-α method	Area $\rho_\$$ [$]	Extended area $\rho_\$$ [$]
BF-3 #1	528.29 ± 9.04	511.67 ± 7.89	0.97699 ± 0.01798	1.12891 ± 0.02847
BF-3 #2	528.90 ± 8.16	525.47 ± 6.55	0.99300 ± 0.01691	1.13125 ± 0.02652
BF-3 #3	532.62 ± 3.41	524.58 ± 2.71	1.00291 ± 0.00762	1.03933 ± 0.01150
Fiber #1	551.62 ± 16.01	518.95 ± 15.28	1.05686 ± 0.03549	1.09990 ± 0.05433
Fiber #2	531.09 ± 6.56	535.64 ± 5.62	0.98490 ± 0.01442	1.03664 ± 0.02193
Fiber #4	538.75 ± 7.94	524.44 ± 7.70	1.00649 ± 0.01879	1.12482 ± 0.02905

Table 4-1-7　　Measured prompt neutron decay constants α [1/s] deduced by PNS and Feynman-α methods

Case 2-D-3 (DT acc.) ($\rho_{pcm, exp}$ = 855.7±41.34 [pcm])				
Detector	PNS method	Feynman-α method	Area $\rho_\$$ [$]	Extended area $\rho_\$$ [$]
BF-3 #1	520.68 ± 14.35	497.98 ± 28.83	0.99970 ± 0.02902	1.10363 ± 0.04398
BF-3 #2	540.67 ± 13.47	513.51 ± 29.28	1.04942 ± 0.02822	1.20361 ± 0.04376
BF-3 #3	539.67 ± 5.94	503.11 ± 19.54	0.99637 ± 0.01220	1.05783 ± 0.01841
Fiber #1	603.37 ± 31.75	644.03 ± 59.61	1.00039 ± 0.05132	1.06198 ± 0.08348
Fiber #2	556.54 ± 12.45	550.18 ± 24.54	0.98282 ± 0.02267	1.08083 ± 0.03559
Fiber #4	526.96 ± 13.58	507.13 ± 36.75	0.98791 ± 0.02879	1.09278 ± 0.04359

Table 4-1-8　　Measured prompt neutron decay constants α [1/s] deduced by PNS and Feynman-α methods

Case 3-D-1 (DT acc.) ($\rho_{pcm, MCNP}$ = 1512.9 ± 5.7 [pcm])				
Detector	PNS method	Feynman-α method	Area $\rho_\$$ [\$]	Extended area $\rho_\$$ [\$]
BF-3 #1	667.29 ± 12.95	626.20 ± 12.85	1.65862 ± 0.04122	1.95981 ± 0.06664
BF-3 #2	655.80 ± 14.14	679.36 ± 15.34	1.72801 ± 0.04526	1.92831 ± 0.07057
BF-3 #3	672.77 ± 5.39	664.35 ± 6.05	1.72456 ± 0.01725	1.90308 ± 0.02698
Fiber #1	673.89 ± 23.09	724.98 ± 38.84	1.60421 ± 0.06756	1.60381 ± 0.10284
Fiber #2	667.31 ± 5.59	661.07 ± 6.15	1.66194 ± 0.01797	1.94418 ± 0.02886
Fiber #3	668.11 ± 11.27	658.91 ± 11.96	1.42546 ± 0.03085	1.65991 ± 0.05085

Table 4-1-9　　Measured prompt neutron decay constants α [1/s] deduced by PNS and Feynman-α methods

Case 4-D-1 (DT acc.) ($\rho_{pcm, MCNP}$ = 3111.6 ± 5.8 [pcm])				
Detector	PNS method	Feynman-α method	Area $\rho_\$$ [$]	Extended area $\rho_\$$ [$]
BF-3 #1	1056.02 ± 38.51	1113.92 ± 41.74	3.73361 ± 0.19036	4.78451 ± 0.34900
BF-3 #2	1119.68 ± 39.02	1064.70 ± 47.73	3.70243 ± 0.18643	5.17838 ± 0.37464
BF-3 #3	1076.31 ± 16.22	1078.63 ± 11.07	3.55740 ± 0.06986	4.26586 ± 0.12752
Fiber #1	1155.278 ± 157.26	1186.20 ± 144.92	-	-
Fiber #2	-	-		
Fiber #4	-	-		

Table 4-1-10　　Measured prompt neutron decay constants α [1/s] deduced by PNS and Feynman-α methods

Case 4-D-2 (DT acc.) ($\rho_{pcm, MCNP}$ = 3111.6 ± 5.8 [pcm])				
Detector	PNS method	Feynman-α method	Area $\rho_\$$ [$]	Extended area $\rho_\$$ [$]
BF-3 #1	1092.18 ± 19.15	999.68 ± 13.50	3.82788 ± 0.06968	5.00179 ± 0.14435
BF-3 #2	1082.50 ± 23.44	1013.01 ± 14.55	3.72918 ± 0.06925	4.51610 ± 0.14738
BF-3 #3	1076.16 ± 24.72	1024.44 ± 5.06	3.90435 ± 0.02899	4.31173 ± 0.11384
Fiber #1	1110.31 ± 56.56	986.93 ± 31.56	3.99660 ± 0.14054	4.59564 ± 0.32699
Fiber #2	1071.20 ± 17.88	993.30 ± 7.48	3.60796 ± 0.04005	4.24635 ± 0.09581
Fiber #4	1063.37 ± 22.56	998.44 ± 15.41	3.85565 ± 0.07871	4.66042 ± 0.15531

Table 4-1-11 Measured prompt neutron decay constants α [1/s] deduced by PNS and Feynman-α methods

Case 4-D-3 (DT acc.) ($\rho_{pcm, MCNP}$ = 3111.6 $\pm$ 5.8 [pcm])				
Detector	PNS method	Feynman-α method	Area $\rho_\$$ [\$]	Extended area $\rho_\$$ [\$]
BF-3 #1	1051.31 $\pm$ 10.10	1000.94 $\pm$ 6.79	3.60407 $\pm$ 0.05694	4.64020 $\pm$ 0.10113
BF-3 #2	1046.19 $\pm$ 10.80	1008.30 $\pm$ 6.44	3.77780 $\pm$ 0.06011	4.66594 $\pm$ 0.10417
BF-3 #3	1073.30 $\pm$ 5.42	1035.34 $\pm$ 2.38	3.76266 $\pm$ 0.02511	4.23217 $\pm$ 0.04311
Fiber #1	1069.91 $\pm$ 22.96	1049.00 $\pm$ 14.85	4.89473 $\pm$ 0.17728	5.05178 $\pm$ 0.25089
Fiber #2	1068.86 $\pm$ 6.59	1003.73 $\pm$ 3.41	3.61753 $\pm$ 0.03547	4.45911 $\pm$ 0.06205
Fiber #4	1065.15 $\pm$ 11.75	1000.72 $\pm$ 7.15	4.10600 $\pm$ 0.07930	5.12115 $\pm$ 0.13295

Table 4-1-12 Measured prompt neutron decay constants α [1/s] deduced by PNS and Feynman-α methods

Case 4-D-5 (DT acc.) ($\rho_{pcm, MCNP}$ = 3111.6 $\pm$ 5.8 [pcm])				
Detector	PNS method	Feynman-α method	Area $\rho_\$$ [\$]	Extended area $\rho_\$$ [\$]
BF-3 #1	1070.93 $\pm$ 14.87	981.40 $\pm$ 17.98	3.48096 $\pm$ 0.08413	4.87113 $\pm$ 0.15607
BF-3 #2	1041.43 $\pm$ 13.38	972.84 $\pm$ 16.43	3.79819 $\pm$ 0.09405	5.40366 $\pm$ 0.16873
BF-3 #3	1067.21 $\pm$ 7.71	995.28 $\pm$ 12.30	3.76012 $\pm$ 0.03970	4.45491 $\pm$ 0.06704
Fiber #1	1061.98 $\pm$ 27.72	1028.16 $\pm$ 34.83	3.77311 $\pm$ 0.16272	4.36965 $\pm$ 0.26057
Fiber #2	1059.13 $\pm$ 10.74	1003.92 $\pm$ 13.44	3.54025 $\pm$ 0.05283	4.27714 $\pm$ 0.09088
Fiber #4	1053.99 $\pm$ 17.86	970.70 $\pm$ 19.62	3.57903 $\pm$ 0.09639	4.81026 $\pm$ 0.17481

Table 4-1-13 Measured prompt neutron decay constants α [1/s] deduced by PNS and Feynman-α methods

Case 5-D-1 (DT acc.) ($\rho_{pcm, MCNP}$ = 5466.8 ± 5.8 [pcm])				
Detector	PNS method	Feynman-α method	Area $\rho_\$$ [\$]	Extended area $\rho_\$$ [\$]
BF-3 #1	1507.29 ± 45.15	1600.24 ± 58.30	13.12317 ± 1.02054	13.12317 ± 1.02054
BF-3 #2	-	-	-	
BF-3 #3	1561.24 ± 16.71	1521.88 ± 11.71	8.04806 ± 0.22314	8.04806 ± 0.22314
Fiber #1	-	-	-	-
Fiber #2	1562.66 ± 25.08	1487.91 ± 22.39	6.74084 ± 0.20170	9.57870 ± 0.41788
Fiber #4	1567.86 ± 41.67	1597.84 ± 77.17	-	-

Table 4-1-14 Measured prompt neutron decay constants α [1/s] deduced by PNS and Feynman-α methods

Case 5-D-2 (DT acc.) ($\rho_{pcm, MCNP}$ = 5466.8 ± 5.8 [pcm])				
Detector	PNS method	Feynman-α method	Area $\rho_\$$ [\$]	Extended area $\rho_\$$ [\$]
BF-3 #1	1542.47 ± 32.10	1531.57 ± 94.15	6.69272 ± 0.26248	9.85874 ± 0.53993
BF-3 #2	1541.73 ± 37.74	1542.69 ± 104.74	7.09606 ± 0.31803	9.58566 ± 0.61002
BF-3 #3	1561.45 ± 12.48	1487.83 ± 19.03	7.12148 ± 0.11291	8.31547 ± 0.18855
Fiber #1	1559.87 ± 70.36	2076.12 ± 339.59	7.68274 ± 0.66021	7.74516 ± 0.96734
Fiber #2	1558.73 ± 18.72	1436.66 ± 39.58	6.44406 ± 0.15399	9.05447 ± 0.30220
Fiber #4	1569.88 ± 36.43	1308.68 ± 110.11	7.70664 ± 0.42332	10.96118 ± 0.77941

Table 4-1-15   Measured prompt neutron decay constants α [1/s] deduced by PNS and Feynman-α methods

Case 5-D-3 (DT acc.) ($\rho_{\text{pcm, MCNP}}$ = 5466.8 $\pm$ 5.8 [pcm])				
Detector	PNS method	Feynman-α method	Area $\rho_\$$ [\$]	Extended area $\rho_\$$ [\$]
BF-3 #1	1518.10 $\pm$ 19.77	1441.77 $\pm$ 14.03	8.60725 $\pm$ 0.25150	11.74861 $\pm$ 0.45170
BF-3 #2	1546.67 $\pm$ 20.78	1420.56 $\pm$ 15.18	8.18430 $\pm$ 0.24169	11.21470 $\pm$ 0.44724
BF-3 #3	1563.35 $\pm$ 9.26	1523.67 $\pm$ 3.69	6.77913 $\pm$ 0.06357	7.54184 $\pm$ 0.11621
Fiber #1	-	1623.23 $\pm$ 44.80	-	-
Fiber #2	1568.87 $\pm$ 13.17	1501.30 $\pm$ 6.54	7.03293 $\pm$ 0.11596	8.79780 $\pm$ 0.21192
Fiber #4	1504.68 $\pm$ 21.32	1381.16 $\pm$ 18.64	19.45768 $\pm$ 1.86598	29.33747 $\pm$ 2.93363

Table 4-1-16   Measured prompt neutron decay constants α [1/s] deduced by PNS and Feynman-α methods

Case 5-D-4 (DT acc.) ($\rho_{\text{pcm, MCNP}}$ = 5466.8 $\pm$ 5.8 [pcm])				
Detector	PNS method	Feynman-α method	Area $\rho_\$$ [\$]	Extended area $\rho_\$$ [\$]
BF-3 #1	1542.40 $\pm$ 26.77	1426.92 $\pm$ 26.99	7.48143 $\pm$ 0.27312	11.76062 $\pm$ 0.57855
BF-3 #2	1591.02 $\pm$ 30.08	1367.56 $\pm$ 28.65	7.67026 $\pm$ 0.31138	12.84927 $\pm$ 0.70248
BF-3 #3	1551.31 $\pm$ 14.62	1513.58 $\pm$ 9.35	7.23510 $\pm$ 0.10362	9.32671 $\pm$ 0.21110
Fiber #1	1608.13 $\pm$ 81.13	1543.68 $\pm$ 77.62	8.70127 $\pm$ 0.71994	11.07538 $\pm$ 1.38422
Fiber #2	1557.72 $\pm$ 18.19	1493.76 $\pm$ 12.89	6.66444 $\pm$ 0.14187	10.45040 $\pm$ 0.32031
Fiber #4	1523.73 $\pm$ 40.46	1434.55 $\pm$ 37.42	9.42282 $\pm$ 0.55816	14.32678 $\pm$ 1.08688

Table 4-1-17　Measured prompt neutron decay constants α [1/s] deduced by PNS and Feynman-α methods

Case 6-D-2 (DT acc.) ($\rho_{pcm, MCNP}$ = 8882.3 ± 5.9 [pcm])		
Detector	PNS method	Feynman-α method
BF-3 #1	-	1780.35 ± 54.79
BF-3 #2	-	2213.13 ± 97.65
BF-3 #3	-	2022.98 ± 16.88
Fiber #1	-	4324.24 ± 1007.21
Fiber #2	-	1703.06 ± 32.53
Fiber #4	-	1926.80 ± 172.55

Table 4-1-18　Measured prompt neutron decay constants α [1/s] deduced by PNS and Feynman-α methods

Case 6-D-3 (DT acc.) ($\rho_{pcm, MCNP}$ = 8882.3 ± 5.9 [pcm])				
Detector	PNS method	Feynman-α method	Area $\rho_{\$}$ [$]	Extended area $\rho_{\$}$ [$]
BF-3 #1	2024.25 ± 61.49	1584.52 ± 128.30	14.92700 ± 1.82496	30.69158 ± 4.60981
BF-3 #2	2144.03 ± 84.83	2023.53 ± 174.81	15.44242 ± 2.04033	32.21389 ± 5.23709
BF-3 #3	2144.99 ± 34.08	1963.84 ± 32.34	12.80783 ± 0.55046	18.95650 ± 1.09303
Fiber #1	1998.46 ± 425.92	1829.06 ± 488.42	12.40719 ± 3.87931	5.56483 ± 2.31382
Fiber #2	1985.47 ± 44.19	1814.45 ± 82.31	12.33320 ± 0.93682	22.10653 ± 2.14379
Fiber #4	2064.13 ± 102.76	2480.72 ± 333.99	16.94444 ± 4.12772	32.17342 ± 8.66792

Table 4-1-19　Measured prompt neutron decay constants α [1/s] deduced by PNS and Feynman-α methods

Case 6-D-5 (DT acc.) ($\rho_{pcm, MCNP}$ = 8882.3 ± 5.9 [pcm])		
Detector	PNS method	Feynman-α method
BF-3 #1	2670.27 ± 125.23	1913.15 ± 270.08
BF-3 #2	3033.82 ± 242.75	3932.08 ± 634.72
BF-3 #3	3067.22 ± 118.67	2419.25 ± 83.22
Fiber #1	2560.30 ± 632.22	5538.75 ± 1156.03
Fiber #2	3148.90 ± 297.81	2914.43 ± 602.96
Fiber #4	2912.04 ± 453.49	5565.46 ± 3640.91

Table 4-1-20　Effective multiplication factor in Cases 2-D (2-F) through 6-D (6-F)

Case	k_{eff} (MCNP6.1 with JENDL-4.0)
Case 1-D (1-F)	-
Case 2-D (2-F); HEU 3000	0.99817 ± 0.00004
Case 3-D (3-F); HEU 2760	0.98400 ± 0.00004
Case 4-D (4-F); HEU 2520	0.96876 ± 0.00004
Case 5-D (5-F); HEU 2280	0.94715 ± 0.00004
Case 6-D (6-F); HEU 2040	0.91747 ± 0.00004

4.2 100 MeV Protons

Table 4-2-1   Measured prompt neutron decay constants α [1/s] deduced by PNS and Feynman-α methods

Case 1-F-1 (FFAG acc.) ($\rho_{pcm, exp}$ = 1352.2 ± 38.82 [pcm])				
Detector	PNS method	Feynman-α method	Area $\rho_\$$ [$]	Extended area $\rho_\$$ [$]
BF-3 #1	689.89 ± 2.07	674.47 ± 1.20	1.41356 ± 0.00273	1.76629 ± 0.00565
BF-3 #2	752.28 ± 1.13	737.51 ± 1.25	1.67789 ± 0.00354	2.10922 ± 0.00611
BF-3 #3	666.36 ± 2.44	653.50 ± 1.25	1.39013 ± 0.00280	1.64844 ± 0.00588

Table 4-2-2   Measured prompt neutron decay constants α [1/s] deduced by PNS and Feynman-α methods

Case 1-F-2 (FFAG acc.) ($\rho_{pcm, exp}$ = 1352.2 ± 38.82 [pcm])				
Detector	PNS method	Feynman-α method	Area $\rho_\$$ [$]	Extended area $\rho_\$$ [$]
Fiber #1	768.70 ± 2.40	771.85 ± 1.71	1.71524 ± 0.00642	1.85089 ± 0.01061
Fiber #2	818.10 ± 2.61	805.01 ± 1.76	1.95777 ± 0.00726	2.20352 ± 0.01242
Fiber #3	784.56 ± 9.17	779.14 ± 2.04	2.00685 ± 0.00454	2.78333 ± 0.02660
BF-3 #1	704.67 ± 2.02	685.23 ± 1.74	1.46667 ± 0.00485	1.84440 ± 0.00859
BF-3 #2	752.37 ± 1.98	741.66 ± 2.07	1.67185 ± 0.00617	2.09335 ± 0.01068
BF-3 #3	688.21 ± 2.32	669.07 ± 1.62	1.49290 ± 0.00513	1.77403 ± 0.00899

Table 4-2-3   Measured prompt neutron decay constants α [1/s] deduced by PNS and Feynman-α methods

Case 1-F-3 (FFAG acc.) ($\rho_{pcm, exp}$ = 2218.9 ± 44.0 [pcm])				
Detector	PNS method	Feynman-α method	Area $\rho_\$$ [$]	Extended area $\rho_\$$ [$]
Fiber #1	1131.56 ± 14.49	1120.19 ± 9.39	2.76157 ± 0.04440	3.12409 ± 0.08529
Fiber #2	1179.28 ± 13.93	1157.56 ± 10.42	3.17980 ± 0.05207	3.68996 ± 0.09821
Fiber #3	1136.05 ± 13.75	1075.86 ± 7.17	3.12964 ± 0.03179	4.92435 ± 0.09021
BF-3 #1	1013.57 ± 4.94	966.32 ± 3.38	2.39188 ± 0.01619	3.38041 ± 0.03348
BF-3 #2	1065.40 ± 5.75	1027.56 ± 4.05	2.66907 ± 0.02091	3.67857 ± 0.04234
BF-3 #3	1026.57 ± 5.74	982.04 ± 3.60	2.55381 ± 0.01960	3.27812 ± 0.03800

Table 4-2-4   Measured prompt neutron decay constants α [1/s] deduced by PNS and Feynman-α methods

Case 1-F-4 (FFAG acc.) ($\rho_{pcm, exp}$ = 2806.8 ± 54.9 [pcm])				
Detector	PNS method	Feynman-α method	Area $\rho_\$$ [$]	Extended area $\rho_\$$ [$]
Fiber #1	1414.12 ± 9.70	1401.96 ± 5.90	3.53790 ± 0.03099	4.16379 ± 0.06793
Fiber #2	1474.29 ± 11.38	1439.92 ± 5.86	3.99097 ± 0.03643	4.72086 ± 0.08298
Fiber #3	1406.26 ± 13.80	1312.41 ± 4.50	3.88047 ± 0.02472	6.25959 ± 0.09960
BF-3 #1	1305.18 ± 6.34	1217.98 ± 4.13	3.06990 ± 0.02139	4.82552 ± 0.05332
BF-3 #2	1353.00 ± 7.60	1290.21 ± 5.22	3.49983 ± 0.02819	5.35192 ± 0.06915
BF-3 #3	1318.24 ± 7.39	1229.44 ± 4.19	3.31538 ± 0.02579	4.66721 ± 0.05952

Table 4-2-5   Measured prompt neutron decay constants α [1/s] deduced by PNS and Feynman-α methods

Case 1-F-5 (FFAG acc.) ($\rho_{pcm, exp}$ = 13254.0 ± 6.1 [pcm])				
Detector	PNS method	Feynman-α method	Area $\rho_\$$ [$]	Extended area $\rho_\$$ [$]
Fiber #1	2735.11 ± 70.62	2972.19 ± 36.03	14.70001 ± 0.47413	14.48612 ± 1.29327
Fiber #2	2548.37 ± 50.17	2375.37 ± 22.69	16.34603 ± 0.53004	22.42986 ± 1.45658
Fiber #3	2549.58 ± 67.04	2357.45 ± 16.72	18.24909 ± 0.50873	30.52158 ± 2.27163
BF-3 #1	2564.35 ± 22.04	2302.49 ± 9.52	11.86773 ± 0.16154	19.42186 ± 0.55781
BF-3 #2	2691.01 ± 45.25	2356.44 ± 21.71	15.75499 ± 0.47618	31.82251 ± 1.82153
BF-3 #3	2844.46 ± 42.48	2455.13 ± 18.55	16.94683 ± 0.45601	31.19015 ± 1.64630

Table 4-2-6　　Measured prompt neutron decay constants α [1/s] deduced by PNS and Feynman-α methods

Case 3-F-1 (FFAG acc.) ($\rho_{pcm, MCNP}$ = 1512.9 ± 5.7 [pcm])				
Detector	PNS method	Feynman-α method	Area $\rho_\$$ [$]	Extended area $\rho_\$$ [$]
Fiber #1	705.96 ± 14.85	719.22 ± 1.29	1.82259 ± 0.00572	2.26361 ± 0.10200
Fiber #2	780.71 ± 27.33	900.39 ± 2.40	5.61627 ± 0.03135	10.24823 ± 0.75562
Fiber #3	800.02 ± 22.21	785.59 ± 2.43	5.76963 ± 0.02645	5.49433 ± 0.37515
BF-3 #1	620.25 ± 2.32	613.23 ± 1.34	1.43617 ± 0.00456	1.75078 ± 0.01056
BF-3 #2	689.60 ± 1.66	675.45 ± 1.39	1.77703 ± 0.00601	2.21869 ± 0.01243
BF-3 #3	579.38 ± 3.13	576.62 ± 1.44	1.32787 ± 0.00428	1.56141 ± 0.01104

Table 4-2-7　　Measured prompt neutron decay constants α [1/s] deduced by PNS and Feynman-α methods

Case 3-F-2 (FFAG acc.) ($\rho_{pcm, MCNP}$ = 2422.6 ± 5.7 [pcm])				
Detector	PNS method	Feynman-α method	Area $\rho_\$$ [$]	Extended area $\rho_\$$ [$]
Fiber #1	1035.20 ± 3.73	1020.68 ± 2.66	2.84329 ± 0.01322	3.56877 ± 0.75391
Fiber #2	-	1303.54 ± 11.94	-	-
Fiber #3	1217.71 ± 10.58	1113.52 ± 3.77	9.07361 ± 0.07213	13.14405 ± 3.65436
BF-3 #1	965.21 ± 15.18	851.50 ± 2.79	2.31917 ± 0.01621	1.54458 ± 0.61125
BF-3 #2	985.52 ± 18.71	934.66 ± 3.39	2.84057 ± 0.02191	2.52729 ± 1.26345
BF-3 #3	968.37 ± 15.18	823.79 ± 2.83	2.19004 ± 0.01526	1.69662 ± 0.61436

Table 4-2-8   Measured prompt neutron decay constants α [1/s] deduced by PNS and Feynman-α methods

Case 3-F-3 (FFAG acc.) ($\rho_{pcm, MCNP}$ = 2714.6 ± 5.7 [pcm])				
Detector	PNS method	Feynman-α method	Area $\rho_\$$ [$]	Extended area $\rho_\$$ [$]
Fiber #1	1153.96 ± 5.91	1132.32 ± 3.60	3.16221 ± 0.02246	4.35512 ± 2.11887
Fiber #2	-	1397.59 ± 5.49	-	-
Fiber #3	1353.14 ± 11.60	1215.37 ± 4.95	10.10259 ± 0.12587	31.62532 ±11.28040
BF-3 #1	1090.15 ± 21.82	953.38 ± 3.41	2.59421 ± 0.01949	4.31016 ± 0.34241
BF-3 #2	1118.92 ± 30.49	1057.83 ± 4.58	3.21619 ± 0.03015	4.63895 ± 0.50563
BF-3 #3	1055.02 ± 18.26	904.09 ± 3.15	2.48810 ± 0.01875	3.98336 ± 0.27902

Table 4-2-9   Measured prompt neutron decay constants α [1/s] deduced by PNS and Feynman-α methods

Case 3-F-4 (FFAG acc.) ($\rho_{pcm, MCNP}$ = 2884.1 ± 5.8 [pcm])				
Detector	PNS method	Feynman-α method	Area $\rho_\$$ [$]	Extended area $\rho_\$$ [$]
Fiber #1	1222.67 ± 8.94	1207.66 ± 5.27	3.23913 ± 0.03420	3.89288 ± 0.06664
Fiber #2	-	1490.87 ± 8.31	-	-
Fiber #3	1454.23 ± 13.44	1285.38 ± 6.34	10.72912 ± 0.20364	20.01503 ± 0.48055
BF-3 #1	1125.12 ± 21.17	1012.46 ± 3.40	2.74824 ± 0.01767	4.25301 ± 0.32784
BF-3 #2	1199.67 ± 26.34	1118.91 ± 4.63	3.40634 ± 0.02744	5.30669 ± 0.51697
BF-3 #3	1139.12 ± 23.54	980.84 ± 3.04	2.63522 ± 0.01704	4.32898 ± 0.36156

Table 4-2-10　Measured prompt neutron decay constants α [1/s] deduced by PNS and Feynman-α methods

Case 3-F-5 (FFAG acc.) ($\rho_{pcm, MCNP}$ = 14785.8 ± 6.1 [pcm])				
Detector	PNS method	Feynman-α method	Area $\rho_\$$ [\$]	Extended area $\rho_\$$ [\$]
BF-3 #1	2232.48 ± 27.73	2019.60 ± 13.07	9.18032 ± 0.18320	17.95485 ± 0.66393
BF-3 #2	2410.92 ± 49.15	2164.72 ± 29.34	13.76546 ± 0.64883	30.58625 ± 2.22143
BF-3 #3	2475.27 ± 39.45	2139.70 ± 18.28	12.30041 ± 0.40731	28.35497 ± 1.56607

Table 4-2-11   Measured prompt neutron decay constants α [1/s] deduced by PNS and Feynman-α methods

Case 4-F-1 (FFAG acc.) ($\rho_{pcm, MCNP}$ = 3111.6 ± 5.8 [pcm])				
Detector	PNS method	Feynman-α method	Area $\rho_\$$ [\$]	Extended area $\rho_\$$ [\$]
Fiber #1	1125.38 ± 3.78	1108.71 ± 2.00	3.61854 ± 0.01663	4.82085 ± 0.03293
Fiber #2	1562.44 ± 8.03	1408.09 ± 3.66	11.70733 ± 0.11908	17.24558 ± 0.23977
Fiber #3	1375.56 ± 9.41	1228.52 ± 3.31	11.30293 ± 0.09279	20.07291 ± 0.26831
BF-3 #1	966.22 ± 6.00	918.48 ± 4.72	2.78717 ± 0.02319	3.77369 ± 0.04428
BF-3 #2	1074.85 ± 6.02	1026.24 ± 4.77	3.59930 ± 0.03212	5.05178 ± 0.06129
BF-3 #3	942.83 ± 6.41	887.37 ± 4.69	2.66206 ± 0.02245	3.49706 ± 0.04260

Table 4-2-12   Measured prompt neutron decay constants α [1/s] deduced by PNS and Feynman-α methods

Case 4-F-2 (FFAG acc.) ($\rho_{pcm, MCNP}$ = 3906.2 ± 5.8 [pcm])				
Detector	PNS method	Feynman-α method	Area $\rho_\$$ [\$]	Extended area $\rho_\$$ [\$]
Fiber #1	1391.13 ± 7.52	1373.04 ± 3.26	4.38045 ± 0.03693	5.64980 ± 0.07543
Fiber #2	1923.49 ± 17.25	1716.23 ± 6.16	14.51611 ± 0.28260	22.32025 ± 0.61495
Fiber #3	1702.94 ± 13.19	1472.83 ± 6.22	13.26441 ± 0.20715	23.86036 ± 0.50561
BF-3 #1	1207.87 ± 10.66	1126.86 ± 7.24	3.42911 ± 0.04326	5.05718 ± 0.09525
BF-3 #2	1330.03 ± 9.58	1243.59 ± 6.73	4.43292 ± 0.05867	6.80633 ± 0.12576
BF-3 #3	1174.22 ± 9.88	1065.23 ± 6.45	3.42483 ± 0.04214	4.81459 ± 0.08743

Table 4-2-13　Measured prompt neutron decay constants α [1/s] deduced by PNS and Feynman-α methods

Case 4-F-3 (FFAG acc.) ($\rho_{pcm, MCNP}$ = 4216.6 ± 5.8 [pcm])				
Detector	PNS method	Feynman-α method	Area $\rho_{\$}$ [$]	Extended area $\rho_{\$}$ [$]
Fiber #1	1510.24 ± 8.97	1496.27 ± 3.55	4.72259 ± 0.03967	5.79531 ± 0.08473
Fiber #2	2057.82 ± 19.03	1864.81 ± 7.14	15.98057 ± 0.31846	24.43068 ± 0.71408
Fiber #3	1869.31 ± 13.40	1603.28 ± 7.06	14.01938 ± 0.22056	26.06993 ± 0.56158
BF-3 #1	1289.31 ± 9.06	1187.38 ± 4.89	3.67468 ± 0.03501	5.55305 ± 0.08255
BF-3 #2	1446.93 ± 8.78	1349.98 ± 4.44	4.94667 ± 0.05298	7.56721 ± 0.11849
BF-3 #3	1297.96 ± 8.56	1163.16 ± 5.11	3.61958 ± 0.03220	5.43031 ± 0.07652

Table 4-2-14　Measured prompt neutron decay constants α [1/s] deduced by PNS and Feynman-α methods

Case 4-F-4 (FFAG acc.) ($\rho_{pcm, MCNP}$ = 4257.9 ± 5.8 [pcm])				
Detector	PNS method	Feynman-α method	Area $\rho_{\$}$ [$]	Extended area $\rho_{\$}$ [$]
Fiber #1	1556.12 ± 8.80	1522.92 ± 3.54	4.81807 ± 0.03981	6.79508 ± 0.09479
Fiber #2	2146.82 ± 19.38	1879.17 ± 3.54	16.81220 ± 0.32995	28.02081 ± 0.81516
Fiber #3	1848.02 ± 13.31	1601.44 ± 7.06	15.06196 ± 0.23488	34.22104 ± 0.71953
BF-3 #1	1287.36 ± 9.06	1188.78 ± 5.19	3.71551 ± 0.04354	5.31464 ± 0.09603
BF-3 #2	1446.88 ± 8.65	1375.82 ± 5.29	5.00395 ± 0.05329	7.66140 ± 0.11927
BF-3 #3	1325.30 ± 9.67	1182.60 ± 5.59	3.61555 ± 0.03216	5.48823 ± 0.08118

Table 4-2-15　Measured prompt neutron decay constants α [1/s] deduced by PNS and Feynman-α methods

Case 4-F-5 (FFAG acc.) ($\rho_{pcm, MCNP}$ = 16947.3 ± 6.2 [pcm])				
Detector	PNS method	Feynman-α method	Area $\rho_\$$ [\$]	Extended area $\rho_\$$ [\$]
Fiber #1	2562.00 ± 76.57	2848.42 ± 21.25	14.36405 ± 0.59092	14.36474 ± 0.59094
Fiber #2	-	2745.70 ± 27.44	-	-
Fiber #3	2911.88 ± 100.32	2686.22 ± 20.70	48.33320 ± 5.21077	80.00728 ±12.21573
BF-3 #1	2277.16 ± 27.08	2022.44 ± 7.29	10.18877 ± 0.18311	15.18345 ± 0.54712
BF-3 #2	2580.40 ± 41.81	2313.12 ± 12.19	19.60222 ± 0.67824	35.40981 ± 2.04051
BF-3 #3	2643.02 ± 35.49	2212.25 ± 11.46	15.90766 ± 0.39806	30.82799 ± 1.43235

Table 4-2-16　　Measured prompt neutron decay constants α [1/s] deduced by PNS and Feynman-α methods

Case 5-F-1 (FFAG acc.) ($\rho_{\text{pcm, MCNP}}$ = 5466.8 ± 5.9 [pcm])				
Detector	PNS method	Feynman-α method	Area $\rho_{\$}$ [$]	Extended area $\rho_{\$}$ [$]
BF-3 #1	1347.72 ± 7.55	1224.98 ± 3.24	4.2409±0.0130	6.6210±0.0557
BF-3 #2	1535.17 ± 3.86	1398.67 ± 4.98	6.4582±0.0254	10.7421±0.0638
BF-3 #3	1302.23 ± 9.671	1123.22 ± 3.32	3.6621±0.0122	5.7880±0.0607

Table 4-2-17　　Measured prompt neutron decay constants α [1/s] deduced by PNS and Feynman-α methods

Case 5-F-2 (FFAG acc.) ($\rho_{\text{pcm, MCNP}}$ = 6283.4 ± 5.9 [pcm])				
Detector	PNS method	Feynman-α method	Area $\rho_{\$}$ [$]	Extended area $\rho_{\$}$ [$]
BF-3 #1	1578.56 ± 8.75	1396.77 ± 4.37	4.9089±0.0238	8.4536±0.0893
BF-3 #2	1757.57 ± 6.66	1578.06 ± 9.59	7.4737±0.0473	13.4353±0.1328
BF-3 #3	1527.84 ± 10.921	1275.66 ± 4.17	4.3431±0.0228	7.5644±0.0959

Table 4-2-18　　Measured prompt neutron decay constants α [1/s] deduced by PNS and Feynman-α methods

Case 5-F-3 (FFAG acc.) ($\rho_{\text{pcm, MCNP}}$ = 6402.4 ± 5.9 [pcm])				
Detector	PNS method	Feynman-α method	Area $\rho_{\$}$ [$]	Extended area $\rho_{\$}$ [$]
BF-3 #1	1634.83 ± 10.43	1440.75 ± 4.85	4.9278±0.0345	8.6750±0.1175
BF-3 #2	1835.08 ± 9.22	1647.52 ± 6.36	7.6800±0.0770	13.3188±0.2001
BF-3 #3	1609.89 ± 11.47	1320.91 ± 4.98	4.3497±0.0328	7.8715±0.1169

Table 4-2-19 Measured prompt neutron decay constants α [1/s] deduced by PNS and Feynman-α methods

Case 5-F-4 (FFAG acc.) ($\rho_{pcm, MCNP}$ = 6449.0 ± 5.9 [pcm])				
Detector	PNS method	Feynman-α method	Area $\rho_\$$ [\$]	Extended area $\rho_\$$ [\$]
BF-3 #1	1668.59 ± 10.09	1457.23 ± 4.78	5.0659±0.0313	9.0312±0.1142
BF-3 #2	1882.18 ± 9.29	1690.14 ± 7.51	7.8179±0.0690	13.7674±0.1928
BF-3 #3	1637.55 ± 11.21	1348.49 ± 5.03	4.4292±0.0294	8.0330±0.1122

Table 4-2-20 Measured prompt neutron decay constants α [1/s] deduced by PNS and Feynman-α methods

Case 5-F-5 (FFAG acc.) ($\rho_{pcm, MCNP}$ = 18537.6 ± 6.2 [pcm])				
Detector	PNS method	Feynman-α method	Area $\rho_\$$ [\$]	Extended area $\rho_\$$ [\$]
BF-3 #1	2395.17 ± 16.79	1953.19 ± 6.48	8.7452±0.0864	17.0252±0.3619
BF-3 #2	2733.48 ± 33.44	2400.04 ± 17.18	22.7337±0.6236	43.2796±1.9802
BF-3 #3	2780.67 ± 26.47	2115.21 ± 9.68	13.4331±0.2333	32.6171±1.1065

Study II

Reaction Rates

Appendix-II
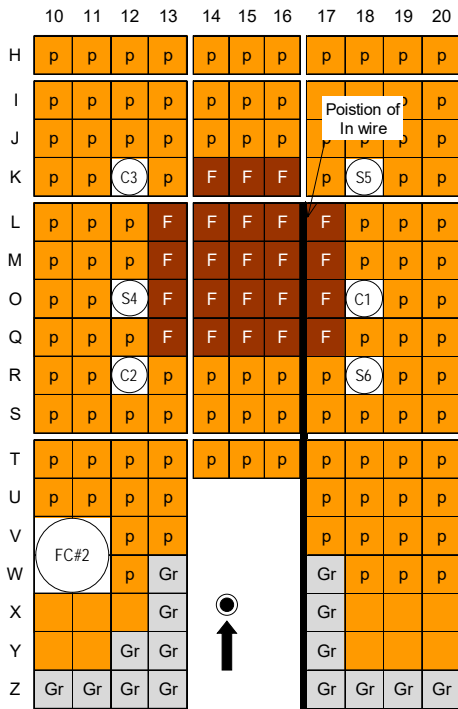
(a) Case 3-D (HEU plates: 2760)   (b) Case 4-D (HEU plates: 2520)
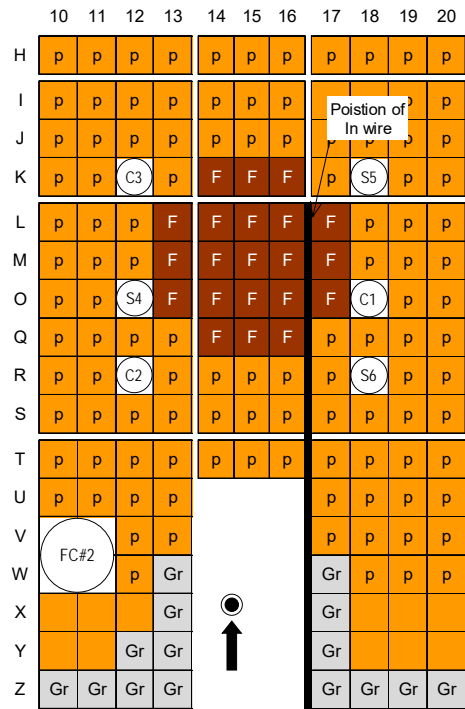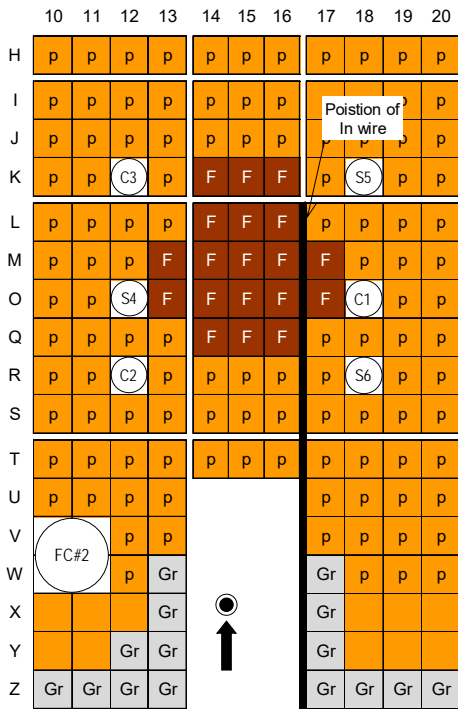
(c) Case 5-D (HEU plates: 2280)   (d) Case 6-D (HEU plates: 2040)
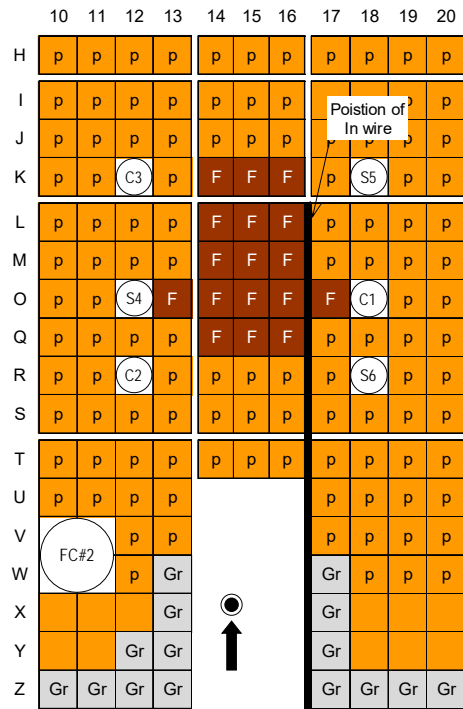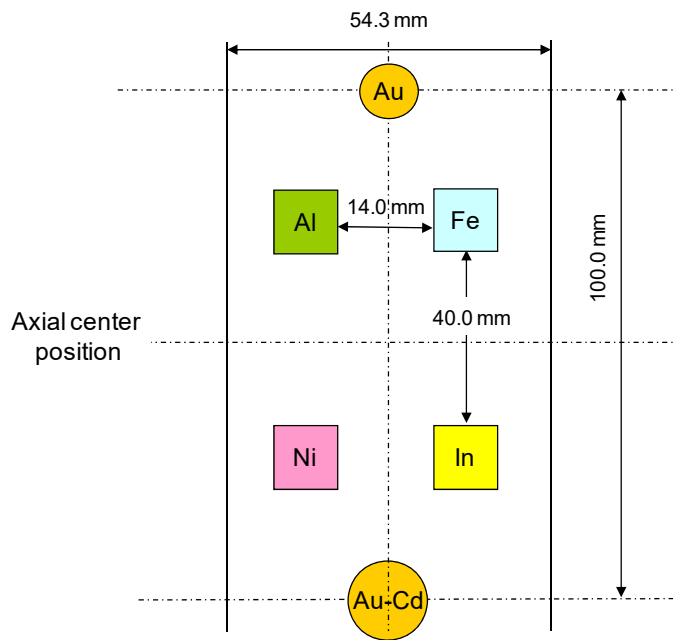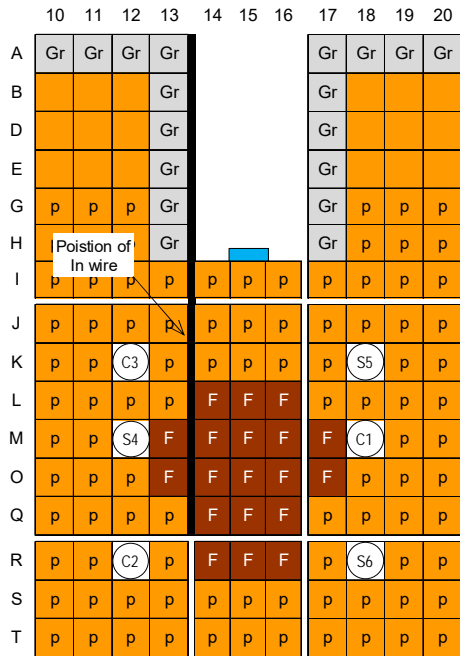
Fig. 5-1   Top view of EE1 ADS core with 14 MeV neutrons.

Fig. 5-2　Foil arrangement at a gap between Pb-Bi target and fuel rod in position (15, M-O) shown in Fig. 4-1

(a) Case 3-F (HEU plates: 2760) (b) Case 4-F (HEU plates: 2520)

(c) Case 5-F (HEU plates: 2280) (d) Case 6-F (HEU plates: 2040)
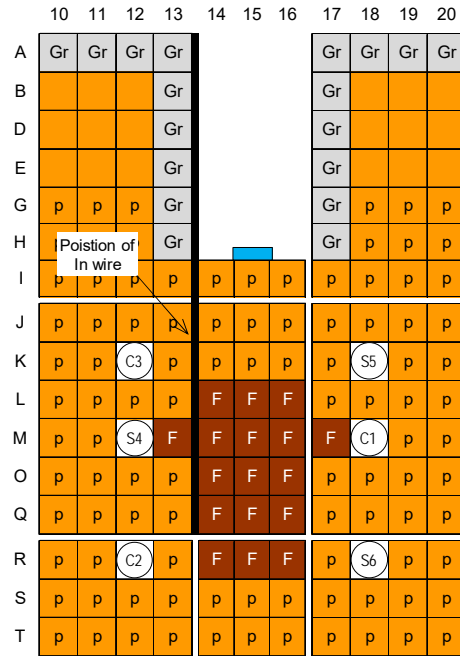
Fig. 5-3   Top view of EE1 ADS core with 100 MeV protons.

5. Results of Experiments
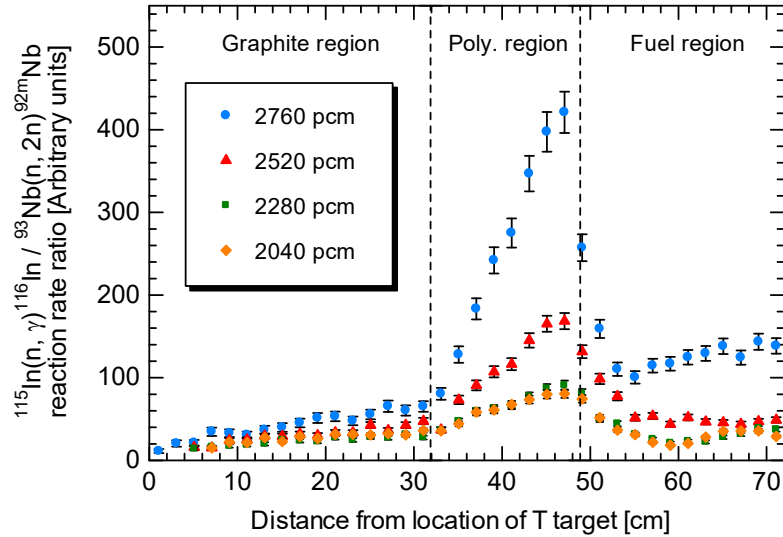
5-1 Indium Reaction Rate Distribution

Fig. 5-1 Comparison between measured ^{115}In(n, γ)^{116m}In reaction rate distributions normalized by ^{93}Nb(n, $2n$)^{92m}Nb along (16-17, L-A') region shown in Figure 1.

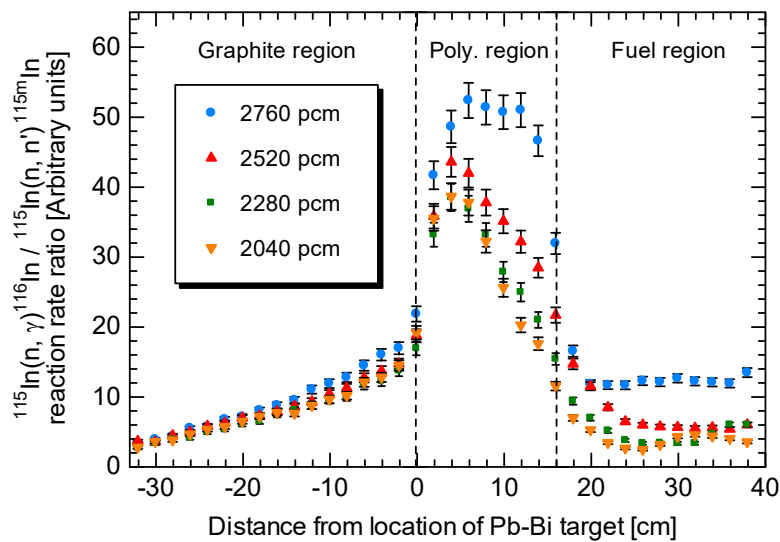Fig. 5-2 Comparison between measured ^{115}In(n, γ)^{116m}In reaction rate distributions normalized by ^{115}In(n, n')^{115m}In along (13-14, A-Q) region shown in Figure 1.

5-2　Reaction Rates of Activation Foils

Table 5-1　Main characteristics and description of activation foils.

Reaction	Dimension [mm]	Threshold [MeV]	Half-life	γ-ray energy [keV]	Emission rate [%]
^{197}Au$(n, \gamma)^{198}$Au (bare and Cd* covered)	8 mm diameter 0.05 mm thick	—	2.697 d	411.9	95.51
Cd plate	10 mm diameter 1 mm thick	—	—	—	—
^{115}In$(n, \gamma)^{116m}$In (wire)	1 mm diameter 680 mm long	—	54.12 m	416.9 1097.3 1293.54	32.4 55.7 85.0
^{115}In$(n, n')^{115m}$In (foil; Pb-Bi target)	10×10×1	0.3	4.486 h	336.2	45.08
^{58}Ni$(n, p)^{58}$Co	10×10×1	0.9	70.82 d	810.8	99.4
^{56}Fe$(n, p)^{56}$Mn	10×10×1	5.0	2.578 h	846.8 1810.7	98.9 27.2
^{27}Al$(n, \alpha)^{24}$Na	10×10×1	5.6	14.96 h	1368.6	100
^{93}Nb$(n, 2n)^{92m}$Nb (T target)	10×10×1	9.0522	10.15 d	934.4	99.2

Cd*: Au foil (Cd covered) was sandwiched between two Cd plates (10 mm diameter and 1 mm thick).

Table 5-2 Atomic density of activation foils utilized in reaction rates measurement.

Foil	Isotope	Abundance (%)	Purity (%)	Atomic density ($\times 10^{24}/cm^3$)
In	^{113}In	4.3	99.99	1.64406E-03
	^{115}In	95.7	99.99	3.66790E-02
Ni	^{58}Ni	68.27	99.0	6.09388E-02
	^{60}Ni	26.10	99.0	2.41006E-02
	^{61}Ni	1.13	99.0	1.06083E-03
	^{62}Ni	3.59	99.0	3.42546E-03
	^{64}Ni	0.91	99.0	8.96354E-04
Fe	^{54}Fe	5.82	99.99	4.83829E-03
	^{56}Fe	91.18	99.99	7.79975E-02
	^{57}Fe	2.1	99.99	1.81771E-03
	^{58}Fe	0.28	99.99	2.46635E-04
^{27}Al	^{27}Al	100	99.0	5.99156E-02
^{93}Nb	^{93}Nb	100	99.99	5.54750E-02
^{197}Au	^{197}Au	100	99.95	5.90193E-02
Cd	^{106}Cd	1.25	99.99	5.39648E-04
	^{108}Cd	0.89	99.99	3.91477E-04
	^{110}Cd	12.51	99.99	5.59564E-03
	^{111}Cd	12.81	99.99	5.78677E-02
	^{112}Cd	24.13	99.99	1.10072E-02
	^{113}Cd	12.22	99.99	5.62419E-03
	^{114}Cd	28.72	99.99	1.33398E-02
	^{116}Cd	7.47	99.99	3.53884E-03

Table 5-3   Measured reaction rates of activation foils in Cases 3-D through 6-D.

Reaction	Measured reaction rate [1/s/cm^3]			
	Case 3-D	Case 4-D	Case 5-D	Case 6-D
^{197}Au$(n, \gamma)^{198}$Au (bare)	(9.657 ± 0.382)E+04	(5.065 ± 0.242)E+04	(3.670 ± 0.150)E+04	(2.051 ± 0.083)E+04
^{197}Au$(n, \gamma)^{198}$Au (Cd)	(6.514 ± 0.310)E+04	(4.083 ± 0.169)E+04	(1.780 ± 0.092)E+04	(2.041 ± 0.087)E+04
^{115}In$(n, n')^{115m}$In	(1.778 ± 0.101)E+02	(2.087 ± 0.109)E+02	(1.331 ± 0.057)E+02	(1.389 ± 0.058)E+02
^{58}Ni$(n, p)^{58}$Co	-	-	-	-
^{56}Fe$(n, p)^{56}$Mn	(8.056 ± 0.665)E+00	(1.895 ± 0.266)E+00	-	-
^{27}Al$(n, \alpha)^{24}$Na	(5.507 ± 0.701)E+00	(2.676 ± 0.473)E+00	-	-
^{93}Nb$(n, 2n)^{92m}$Nb (T target)	(2.801 ± 0.114)E+02	(4.765 ± 0.176)E+02	(6.652 ± 0.297)E+02	(6.533 ± 0.260)E+02

Table 5-4　Measured reaction rates of activation foils in Cases 3-F through 6-F.

Reaction	Measured reaction rate [1/s/cm^3]			
	Case 3-F	Case 4-F	Case 5-F	Case 6-F
^{197}Au$(n, \gamma)^{198}$Au (bare)	(5.443 ± 0.180)E+06	(2.715 ± 0.090)E+06	(1.585 ± 0.053)E+06	(1.104 ± 0.036)E+06
^{115}In$(n, n')^{115m}$In	(1.671 ± 0.060)E+04	(0.842 ± 0.030)E+04	(0.518 ± 0.019)E+04	(0.401 ± 0.014)E+04
^{58}Ni$(n, p)^{58}$Co	(1.582 ± 0.071)E+04	(0.777 ± 0.029)E+04	(0.506 ± 0.019)E+04	(0.380 ± 0.015)E+04
^{56}Fe$(n, p)^{56}$Mn	(3.415 ± 0.195)E+02	(2.027 ± 0.121)E+02	(1.326 ± 0.077)E+02	(1.921 ± 0.074)E+02
^{27}Al$(n, \alpha)^{24}$Na	(6.696 ± 0.408)E+02	(3.110 ± 0.163)E+02	(1.155 ± 0.099)E+02	(1.291 ± 0.053)E+02
^{115}In$(n, n')^{115m}$In (Pb-Bi target)	(1.900 ± 0.060)E+05	(1.947 ± 0.062)E+05	(2.194 ± 0.068)E+05	(2.160 ± 0.068)E+05